

**A study of spike-triggered EEG waveforms based on automated surface
EMG decomposition of muscle activity comprising primal and fine hand
movements**

Damian Machlanski

A thesis submitted for the degree of Master of Science in Artificial Intelligence

Supervisor: Dr. Ana Matran-Fernandez
Co-supervisor: Prof. Luca Citi
School of Computer Science and Electronic Engineering
University of Essex

August 2020

Abstract

The latest advances in biomedical signal processing have enabled new research avenues, such as robotic hand prosthesis. It is believed the investigation of both complex finger control and simple gestures based primarily on muscle force could be beneficial to the development of dexterous prostheses. Although fine hand movements have been studied in the past to some extent, the research was almost exclusively concentrated on corticomuscular coherence analysis, which has certain limitations. Encouraged by recent successes of High-Density surface electromyography (HDsEMG) decomposition methods, this study attempted to perform the analysis on the level of a single Motor Unit (MU) by incorporating simultaneously recorded HDsEMG and electroencephalography (EEG) signals. For this purpose, a K-means Convolution Kernel Compensation (KmCKC) decomposition algorithm was first replicated and validated on simulated HDsEMG signals. Then, using the implemented method, the experimental HDsEMG recordings were decomposed into constituent MUs. 225 extracted units were then tracked across subsequent trials to form 46 common sources, all of which were utilised to generate 46 EEG Event-Related Potentials (ERP) related to motor cortex brain area. According to the obtained results, no consistent ERPs were detected in the expected time lag (15 ms) before the triggering event. Furthermore, no significant discrepancies between the investigated hand movement types were observed in the produced EEG waveforms. However, these outcomes may merely reflect the limitations of the employed methodology or the need to inspect brain regions outside of motor cortex, both providing directions for future work.

Keywords— finger control, high-density surface EMG, convolution kernel compensation, event-related potentials.

Contents

1	Introduction	1
2	Background	2
2.1	Decomposition of sEMG	3
2.1.1	General Background	3
2.1.2	Methods	4
2.2	Related Work	7
2.2.1	sEMG Decomposition of Hand Muscles	7
2.2.2	Joint Analysis of Brain and Muscle Signals	8
2.3	Research Questions	10
2.4	Goals and Objectives	11
3	Methodology	12
3.1	Data	12
3.1.1	Simulated Data	12
3.1.2	HDsEMG and EEG	13
3.2	Decomposition	13
3.2.1	Data Model and CKC	14
3.2.2	Pre-Processing	18
3.2.3	KmCKC	20
3.2.4	Post-Processing	23
3.3	Evaluation	27
3.3.1	Implementation Stage	27
3.3.2	Real Recordings	28
3.4	Tracking Common Motor Units	28
3.5	Spike-Triggered EEG Waveforms	31
3.6	Overview and Parameters	31
4	Implementation of KmCKC algorithm	33
4.1	Challenges	33
4.2	Experimental Modifications	36
4.3	Validation of KmCKC Implementation	37
4.4	Discussion	37
5	Joint Analysis of HDsEMG and EEG	39
5.1	Decomposition	39
5.2	Common Sources	40
5.3	EEG Event-Related Potentials	42
5.4	Discussion	43
6	Discussion	48
7	Conclusions and Future Work	50
8	References	52

1 Introduction

Recent developments within the field of biomedical signal processing have enabled new practical applications and previously unexplored research directions. These great advances can be usually attributed to either more sophisticated hardware or software. With regards to the former, it means better acquisition instruments that lead to more accurate data collection. Moreover, increased compute power available allows for more complex settings and overall provides faster processing. Likewise, more advanced software facilitates efficient calculations and allows to tackle increasingly difficult and novel problems.

One of the new aforementioned possibilities is hand prosthesis, which aims to provide a synthetic hand for amputees, controllable through physiological signals. Although many great inventions have been proposed already (e.g., [1, 2]), there are still problems that need to be addressed, such as intuitiveness, adaptiveness and real-time control [3]. One of the ongoing projects, DeTOP [4], specifically aims at improving upper limb prosthesis solutions, to give an example.

What perhaps could help with hand prosthesis is investigating a possible difference between two types of hand movements: a) the ones developed by humans over time that usually require delicate precision and high complexity, and b) those shared among humans and other primates, which primarily involve muscle force instead. Both types of gestures are henceforth referred to as fine and primal hand movements respectively. Furthermore, this type of difference is hypothesised to be exhibited in the motor cortex of the brain as hand muscle contractions are expected to activate this region [5], but perhaps with slightly different Event-Related Potential (ERP) timings or even a different way they originate from the brain to the arm. Thus, if this is indeed the case, there is a chance that investigating brain signals, while those hand movements were performed, could reveal some discrepancies. In case this phenomenon can be confirmed, some further questions arise, such as whether the difference is significant and universal across experimental sessions and subjects, or how this anomaly is actually exhibited in brain signals.

In fact, this research direction has been initially investigated in a preliminary study [6], wherein, despite promising signs, it became clear that a more thorough investigation was needed to confirm the significance of obtained results. This initial progress definitely encourages further work within the problem, which is the main source of motivation of this study and can be considered its departure point.

One possible way of tackling this problem is to collect and analyse both electromyography (EMG) and electroencephalography (EEG) signals simultaneously while performing the aforementioned hand movements. Although some existing works attempted to do a similar joint analysis, they were usually focused on different hand gestures and then performed coherence analysis at the end. As much as the standard EMG-EEG coherence can be considered a useful tool, it is hampered by the fact that the neural drive to muscle within EMG signals is contaminated by the electrical properties of muscle fibres [7]. In order to avoid the drawbacks of coherence analysis, this study attempts to directly investigate EEG waveform shapes in the time domain, which

hopefully would provide some new valuable information. More precisely, the idea is to decompose High-Density surface EMG (HDsEMG) into discharge times of active Motor Units (MUs) and consequently use them to produce EEG ERPs, with the aforementioned discharge patterns utilised as events. Interestingly, it appears this specific approach is something that no other study has ever tried before, making it a novel strategy to the joint analysis of EEG and EMG signals, introduced as part of this work.

There are many techniques of obtaining said spike trains of active MUs out of muscle signals, which vary depending on the invasiveness of the recordings. Due to recent hardware developments, it is now possible to incorporate tens or even hundreds of electrodes to collect electrical activity of different muscles from the surface of the skin through HDsEMG grids. On top of that, the latest algorithmic advances have delivered automated decomposition methods capable of extracting the information about the underlying sources from HDsEMG signals. It is fair to point out that HDsEMG decomposition still requires further work, but nevertheless it already provides useful solutions (e.g., [8, 9, 10]) and is a promising means of advancing prosthesis control [3, 11]. Given the benefits of HDsEMG and available decomposition algorithms, this project attempts to explore and combine both in order to obtain discharge patterns of active MUs from HDsEMG that are needed for further EEG analysis.

However, there is a noticeable difficulty with regards to HDsEMG decomposition as there are no publicly available implementations of said algorithms. This fact, in turn, raises some doubts why this would be the case. It could be due to a plain high difficulty of the implementations, or because of unclear descriptions hampering replication. Regardless of the reason, it is difficult to compare the methods to each other and choose the best one for a given use case as a consequence. Thus, it is believed that replicating one of the latest decomposition techniques has a chance of having a positive impact on the community, and hence constitutes one of the goals of this work.

Given the above discussion and identified gaps, this work offers the following contributions:

- Replication of a state-of-the-art HDsEMG decomposition algorithm.
- A novel approach to the joint analysis of EEG and HDsEMG based on extracted discharge patterns and EEG ERPs.
- The investigation of differences between primal and fine hand movements exhibited in EEG waveforms.

2 Background

This section gives a comprehensive review of the background information suitable for the project at hand (Section 2.1) and contextualises this study within existing research (Section 2.2). Furthermore, the research questions this work aims to answer are discussed (Section 2.3), which are in turn directly linked to goals and objectives

of this project (see Section 2.4).

2.1 Decomposition of sEMG

The following subsection offers a brief discussion of the general aspects of surface EMG (sEMG) decomposition (Section 2.1.1), followed by a review of common decomposition algorithms (Section 2.1.2). However, before going into details, it might be worth distinguishing between spike sorting and decomposition methods as they can be considered closely related and hence cause confusion. As pointed out in [12], spike sorting, a set of techniques widely used in computational neuroscience, happens at the level of the nerves. These approaches are indeed quite similar to intramuscular EMG decomposition methods as they target selected muscle fibres. This is certainly not the case in surface EMG, where the electrodes are located on the surface of the skin and thus are relatively distant from the underlying muscle fibres. This project is exclusively focused on sEMG decomposition methods due to the chosen methodology, and only those are discussed in the following subsections.

2.1.1 General Background

General background on sEMG decomposition and the analysis of motor units is comprehensively discussed in [13]. As the authors point out, surface EMG can be preferred over intramuscular settings (iEMG) when the latter is undesirable or not possible, due to the risk of infections, overall patients' discomfort or the need for surgeries to place the needles. Surface electrodes, on the other hand, can be used with ease, even for non-clinical cases. The study also highlights the fact that invasive solutions have been the default approach for many years, which to a great degree is completely understandable as iEMG has its advantages. For instance, it is good for inspecting single MUs, although due to its high selectivity the number of identified sources is limited.

When it comes to surface EMG, the MUAP shapes of detected sources are much more similar to each other, especially when very few electrodes are employed [14]. As it is desirable to identify as many different motoneurons as possible, it is important to decrease the degree of similarity across obtained sources. To counteract this issue, multiple closely-spaced surface electrodes are employed, enabling the detection of various underlying sources. An approach incorporating such a set of electrodes is often called High-Density surface EMG, organised as two-dimensional electrode grids. Some of the drawbacks of this technique involve heavy data caused by a high number of channels or the fact that through this technique only superficial sources that are close to the skin are detected. Nevertheless, encouraged by early successes, HDsEMG approaches have quickly become a new, rapidly evolving field, comprising new acquisition and processing methods. For a detailed review on those two aforementioned aspects refer to [14].

Furthermore, sEMG decomposition can be used to decode the neural drive to muscles [15]. The usual approach based on the signal's amplitude can be inaccurate, whereas recent sEMG decomposition methods provide discharge times of identified MUs, which are much more reliable, although they are usually limited to isometric

contractions and detect superficial units. Thus, for a complete muscle activity information, there might be a need to utilise intramuscular recordings as well. Moreover, [7] argues that spectral, amplitude and coherence analysis are limited, despite their popularity. Given recent advances in sEMG decomposition, using discharge times is more reliable as it provides direct information about the neural drive to muscles. Besides, it has been shown that HDsEMG decomposition can reliably estimate motor unit properties within and across sessions, handling ranges of 10-70% Maximum Voluntary Contraction (MVC) [16].

A very recent account of the up-to-date practices and recommendations within sEMG is provided in [17], which also expands further on HDsEMG decomposition specifically. The report offers a rich discussion on the topics of acquisition, inspection, decomposition, analysis and interpretation of HDsEMG. It is worth noting that the authors specifically point out that as of today the usual decomposition process is rather semi-automatic, and that decomposition results should be carefully inspected afterwards. This is rather contrary to how most decomposition algorithms are described in their respective publications as they are often said to be fully automated. Apart from that, [17] argues the biggest limitation of current decomposition techniques is their variable performance across muscles and subjects.

Finally, despite all the aforementioned limitations of today's sEMG decomposition techniques, they are very promising. In fact, there were attempts to use them under non-stationary conditions [18]. In addition, sEMG is considered to be a viable solution towards better upper-limb prostheses [3].

2.1.2 Methods

As pointed out in [14], there are two main approaches to sEMG decomposition: template matching and Blind Source Separation (BSS).

Template Matching. The approach tries to identify and match MUAP templates, which is closely related to intramuscular EMG decomposition. However, these methods struggle to separate superimposed action potentials and hence provide incomplete discharge patterns. This problem is indeed highlighted in [19], which mentions that full discharge patterns are obtained only in some specific cases.

Blind Source Separation. There are two commonly used data models in BSS: instantaneous and convolutive [14]. The former is overly simplistic as it ignores important anatomical characteristics, whereas the latter accounts for that complexity and is much more useful in practice. In addition, the convolutive mixing model does not rely on MUAP shapes and hence can separate overlapping ones, enabling the extraction of full discharge patterns. Its major downside is the assumption of no, or at most weak, correlation between sources. On the other hand, it does not assume any muscle architecture and allows for different MUAP shapes across channels.

There are two main approaches within BSS: methods based on either Independent Component Analysis (ICA) algorithm or Convolution Kernel Compensation (CKC). ICA methods generally aim to approximate the unmixing matrix, that is, the opposite of the (unknown) mixing matrix used during the mixing process of the original

sources. Once the unmixing matrix is obtained, the mixing process can be reverted. In the context of sEMG decomposition, the unmixing matrix is combined with all the observations in order to get the original sources. One of the initial investigations of using ICA in the sEMG domain was not successful [20], where the authors analysed the performance of sparse ICA. Nevertheless, despite this initial setback, a Progressive FastICA Peel-off (PFP) framework [21], primarily based on the FastICA algorithm [22], finally provided a viable ICA-based solution for sEMG decomposition. The two major improvements that PFP offers over previous FastICA-based decomposition methods are: a) PFP incorporates the convolutive mixing model, and b) PFP solves the FastICA convergence problem. This work was further extended in [23] into a completely automatic framework, which was then validated against simultaneously recorded intramuscular and surface EMG [24], also known as a two-source method.

Another branch of BSS methods focuses specifically on the convolutive mixing model of the sEMG. After initial investigations of correlations [25] and higher-order statistics [26] within sEMG decomposition, the CKC method was finally introduced in [8], offering the extraction of complete discharge patterns. Instead of approximating the unmixing matrix, the CKC method iteratively identifies discharge times of a single source through which it finally extracts a complete Innervation Pulse Train (IPT). The method operates directly on spike trains, which greatly helps with addressing the MUAP superposition problem. As a consequence, the MUAP shapes are lost in the middle of the process, though they can be restored through Spike-Triggered Averaging (STA) [27] using the times of the spikes in the IPTs. The CKC was further extended in [28] into gradient CKC (gCKC) by utilising a gradient-based optimiser to improve the quality of reconstructed sources, although the choice of cost functions for the optimiser is not a trivial task [29] and can severely affect the quality of the decomposition.

As the original study that introduced CKC method validated it on artificial datasets only, there was certainly a need to test its capabilities more thoroughly. Thus, both classic CKC and gCKC approaches have been since extensively validated via the two-source method, involving different MVC levels [30, 31] and pennate muscles [32]. Moreover, CKC techniques have been applied to many real-world settings, including force estimation [33], pathological and essential tremor [34, 35, 36], targeted muscle re-innervation [2], dynamic muscle contractions [37], prostheses control [11], tetraplegia after spinal cord injury [38] and various hand muscles [39]. Furthermore, the CKC approach has been compared to other decomposition methods, such as PFP [40] and non-negative matrix factorisation [41].

Encouraged by the aforementioned successes, CKC algorithm has quickly become a promising baseline for further extensions. Perhaps one of the biggest issues of current decomposition methods is the fact that they are not suitable for online solutions. Thus, some studies attempted to incorporate CKC into a real-time framework [42, 43, 44]. Many studies also investigated the feasibility of combining clustering methods together with CKC, for instance, Fuzzy C Means [45], waveform clustering [46] or K-means [9]. The latter, proposing a K-means CKC (KmCKC) method, is specifically interesting

due to it introducing an iterative refinement procedure that markedly improves source estimation. Despite a relatively simple and greedy approach behind the improvement loop, it indeed seems to be providing reliable results, as demonstrated in the works that applied the method to real-world problems [47, 48, 49].

Other Methods. Apart from the two classic approaches to sEMG decomposition, that is, template matching and blind source separation, there have been attempts to combine them, or even go beyond standard techniques. As no algorithm is ever free from weaknesses, those algorithmic hybrids usually aim at combining the strengths of the methods at hand, resulting in a more accurate decomposition. One of the examples is the work presented in [50], wherein template matching is integrated with ICA. The main motivation there is to address the most prominent weakness of the former, which is its inability to fully separate superimposed MUAPs. Therefore, the proposed remedy is to separate sources first through a modified ICA and then proceed with template matching as usual. The results are indeed encouraging as the introduced solution successfully extracted quality sources from contractions of up to 60% MVC.

Another mixed approach incorporating template matching combined it with gCKC [12], where the latter is rather its central point. The method, called Guided Source Separation (GSS), first detects and clusters MUAPs (template-based part), which in turn serves as initial point information for a modified gCKC. The framework also introduces a soft-thresholding procedure for extracting peaks from IPTs, pushing the performance of the method even further. Overall, when compared to vanilla gCKC, GSS managed to find more sources, however, at the cost of slightly worse accuracy.

Following further with hybrid methods incorporating CKC, some approaches attempt to integrate it with other BSS algorithms. One such investigation was done in [10] that mixes some ideas from both FastICA and gCKC. The resulting technique is capable of decomposing surface as well as intramuscular recordings, a rare trait among decomposition methods. The proposed procedure was thoroughly tested, results of which were compared to manual decompositions performed by experienced operators. The reported performance does look impressive as the method successfully detects many sources within a wide range of MVCs (10-90%). Also, it is worth highlighting that among many articles proposing sEMG methods this work is perhaps one of the most informative ones, mostly due to discussing not only the algorithm itself but also pre and post-processing steps involved, which are critical for replication and yet neglected in countless other works within the field.

Some other sEMG decomposition methods go even beyond standard template-based or BSS techniques. For instance, a relatively common Precision Decomposition III (PD III) procedure, introduced in [51] and extended in [52], is based on Artificial Intelligence (AI) methods at its core and offers two modes of operation: automatic and interactive. Although PD III delivers truly outstanding outcomes, it is rather designed to work on relatively few surface electrodes, rendering it unsuitable for studies wanting to investigate HDsEMG settings. Another work outside of classic approaches involves Measurement Correlation (MC) and Linear Minimum Mean Square Error (LMMSE)

[53], which, although quite different on the surface, appears to have some similarities with CKC and ICA techniques as well. Its main features are different initialisation of the correlation matrix and an advanced iterative procedure correcting obtained IPTs. The latter aspect resembles to some extent the refinement loop proposed in KmCKC, though MC-LMMSE offers a definitely more complex solution here. Another method employing AI techniques is presented in [54], which trains a recurrent neural network in a supervised manner on the outputs given by gCKC. Interestingly, the proposed deep learning-based method outperformed vanilla gCKC on the signals with low signal-to-noise ratio, while being much faster at the same time.

2.2 Related Work

This section discusses past works related specifically to the main goals of this study, that is, a) to decompose HDsEMG of hand movements, and b) to generate and analyse EEG ERPs based on spike trains extracted in (a). While some research has been done in the past with regards to (a), there is no evidence of any attempts that would relate directly to (b). This is because this project is the first documented attempt of performing this novel type of analysis. As a result, the selected past research that is being discussed in the context of (b) does not answer the same questions as this work, but can be still considered related, at least to some extent.

2.2.1 sEMG Decomposition of Hand Muscles

This subsection discusses past research employing sEMG decomposition specifically in the context of hand manipulations. Although post-decomposition analysis of presented studies may differ from this work, the decomposition part of the methodology is indeed relevant.

Many past investigations of the hand based on sEMG recordings primarily utilised crude signals or global characteristics (see [1, 55, 56] for examples). Inspired by recent advances in sEMG decomposition, as discussed in Section 2.1, an alternative approach has arisen that constitutes of extracting discharge times of underlying motor units and then proceeding with further analysis.

One example of this approach is presented in [57], where the decoded neural activity was successfully used as control signals for a prosthetic hand, though not specifically in the context of finger movements but wrist kinematics instead. Although the proposed solution cannot be applied to real-time problems, this direction proved to be promising, especially as it offers as many as three degrees of freedom in terms of wrist control. The work was further extended in [11], which this time incorporated dimensionality reduction and linear regression to predict wrist movements. Similar work was done as part of [58], where the wrist kinematics was also investigated, although in the context of post-stroke rehabilitation. The authors showed that one of the commonly used approaches, that is, sEMG envelopes, can be rather inaccurate, whereas the proposed technique based on sEMG decomposition is much less sensitive to the distribution and shapes of detected sources.

Furthermore, apart from wrist-based works, there have been studies that focused

specifically on finger movements. One such an example, presented in [59], employed decomposition and further a first principal component to successfully predict continuous finger movements. As pointed out by the authors, the proposed method outperformed previous approaches based on global EMG features, proving again the effectiveness of sEMG decomposition and giving future perspectives for a dexterous prosthesis.

Finally, a very recent piece of research, and which can be considered the closest to this work in terms of sEMG decomposition, was done as part of [39]. The study involves recordings of hand and forearm muscles comprising a wide range of hand movements. In fact, two of the inspected gestures relate specifically to the ones investigated in this project (pinch and grip). One of the interesting aspects of the work is the post-processing performed right after the decomposition that sheds some light on the physiological properties of hand muscles that should be reflected in decomposed motor units. Overall, the study proves the feasibility of investigating various hand movements through HDsEMG decomposition.

2.2.2 Joint Analysis of Brain and Muscle Signals

As aforementioned, this study is the first reported attempt to analyse EEG STAs based on pulse trains obtained from HDsEMG while performing specific hand movements. For this reason, no past research exactly matches these efforts. However, there is still a subset of research that jointly analysed brain and muscle recordings within the context of hand movement complexity, which is indeed of interest for this project. The major discrepancy lies in the employed methods of analysis, as all the past work within this topic was concentrated on coherence analysis, whereas this study investigates spike-triggered EEG waveforms. The two approaches are significantly different as they happen in the frequency and time domain respectively. This work does not attempt to perform coherence analysis, but those past works that inspected hand movement complexity based on brain and EMG signals are considered relevant nevertheless, despite some discrepancies in employed methodologies.

Before discussing the hand movement complexity analyses within both brain and muscle signals, it is worth starting the topic from a perspective of whether and how the brain signals are actually synchronised with EMG recordings of the hand muscles. This direction was to some extent investigated in [60], although the work focused specifically on the relationship between spike train timings of different motor units. The authors show the association between such neurons can be effectively measured through coherence of the discharge times of their spike trains. Moreover, it was shown there that if a high coherence between the timings of spike trains of a pair of motoneurons can be found, it is then entirely due to the presence of a common input those neurons receive. This is highly important as it proves the existence of the common drive to the muscle.

Furthermore, the study in [5] specifically investigated the synchronisation between motor cortex and spinal motoneurons under constant isometric contractions at less than 10% MVC. First, the study confirmed that hand muscle contractions correspond to the contralateral motor cortex area. But more importantly, they showed through

coherence between motor cortex and muscle signals that cortical activity directly contributes to the frequencies at which pairs of motor units were previously found to be strongly associated together (16–32 Hz). In other words, the implication is that motor cortex is one of the common sources that drives hand muscles, first dorsal interosseous in this case, though the authors also highlight that motor cortex is likely not the only common source influencing these muscles.

Finally, the work in [61] investigated both upper and lower limbs in the context of corticomuscular synchronisation within a wide range of MVCs (maximal, moderate, and weak contractions). The authors found the coherence peak at around 45 Hz for maximal and moderate MVCs, and at 20–30 Hz for weak contractions. On top of that, it has been shown that cortical activity precedes the EMG one, and that the time lag is constant regardless of the MVC involved (mean lag of 4.21 ms in the range of 2–8 ms for the hand muscles inspected). Moreover, the relationship between the contralateral cortex and activated muscles has been again confirmed, which agrees with the previously discussed study ([5]).

With regards to hand movement complexity, the study in [62] investigated simple and complex sequential finger movements, where all the hand fingers were involved. The authors incorporated Position Emission Tomography (PET) to inspect the blood flow of the brain during experiments. Furthermore, they showed that some specific brain regions exhibited the most increase in activation by shifting from simple to repetitive movements, whereas other areas showed a significant raise only when switching to complex sequences. Overall, the main takeaway is that certain discrete areas of the brain are activated during sequential finger movements. In other words, complex finger movements activate very specific brain regions, where some of them are attributed to memory and planning functions while the other to the actual execution of the movement. This suggests the motor cortex is not the only region strongly related to fine finger control. Although this heavily depends on how complexity is defined, which is attributed to sequence length (i.e., number of movements) in this study, which indeed is sensible as authors highlighted the fact that the rate of incorrect finger movements increased with the sequence length.

Another research investigating complex hand movements by inspecting brain's blood flow through PET is presented via [63]. The experiments involved either both hands at the same time or each in separation. The study offers two main takeaways: a) complex finger movements activate certain brain regions bilaterally (primary motor areas, premotor areas and cerebellum), which was in contrast to supplementary motor area that was activated by contralateral movements, and b) premotor area might be important in learning motor skills. With regards to a) the authors point out that this is indeed in contrast to other studies, but this report studied different hand movements, suggesting that the definition of what constitutes a complex hand movement is of crucial importance here, and hence might be the source of discrepancies across studies. Thus, it appears that whether complex hand manipulations are organised unilaterally or bilaterally depends on the investigated movement type.

Furthermore, the study in [64] analysed isometric contractions of upper and lower limbs through magnetoencephalography (MEG) and sEMG signals. First finding is

that there is a significant activity in the primary motor cortex (M1) contralateral to the contracted muscle. Secondly, the coherence peak between rectified EMG and M1 was found to be at 20 Hz across all subjects, which is in agreement with previous studies. Thirdly, the time lag between M1 and EMG, which was in agreement with conduction times, was very consistent and hence M1 indeed drives the motor unit pools. The last finding is in line with [5] that MEG and sEMG are coupled, though [5] found a lag of zero between them, whereas [64] argues there is a non-zero lag and thus concluding it is not a peripheral feedback but rather a cortical drive to the muscle. Furthermore, the time lags reported in [64] are much higher than those suggested in [61], where the former performed much more thorough and sound analyses in this matter. For instance, the lag for extensor indicis was reported to be around 15 ms.

There is also a series of studies that, although did not investigate hand movement complexity, jointly analysed EMG and EEG signals within the context of corticomuscular coupling, which is certainly of interest for this project as well. One such an example is demonstrated in [65], where a corticomuscular coherence has been found between rectified EMG and EEG at the tremor frequency in essential tremor. This finding contrasts with previous research employing MEG that could not find significant coherence in essential tremor, rendering simultaneous recordings of EMG and EEG as a powerful tool for this type of analysis.

Furthermore, Negro and Farina showed that cortical input is linearly transmitted to motoneuron pools, and that also some non-linearities are introduced by the motoneurons themselves [66]. This is indeed in line with previous studies that inspected the neural drive to muscle, but the authors also offer thorough mathematical derivations to support the conclusions. It is also worth noticing that the authors approached the problem a bit differently when compared to previous research. More concretely, they decomposed sEMG signals into constituent motor unit spike trains, which were then aggregated into a Cumulative Spike Train (CST). Finally, they analysed CST-EEG coherence to study the cortical drive to the muscle. This proves again the power of sEMG decomposition. A similar approach was taken in [67], though in the context of essential tremor, which showed an increased synchronisation in essential tremor patients. Encouraged by the successes of the new CST-based methodology, the study in [36] inspected CST-EEG coherence within pathological tremor. The new approach indeed proved to be more precise than the usual method involving EMG-EEG coherence, showing once again the new possibilities provided by HDsEMG decomposition.

2.3 Research Questions

Given the discussion so far and identified new possibilities and gaps, the following questions arise:

- Q1: What are the challenges of HDsEMG decomposition?
- Q2: Can we detect ERPs in motor cortex areas that arise before the occurrence of spikes?
- Q3: Are there any significant differences between primal and fine hand movements exhibited in EEG waveforms?

In terms of Q2 and Q3, the studies investigating the neural drive to muscle clearly show the existence of a consistent time lag between cortical signals and motoneuron pools [60, 5, 61, 66]. Moreover, it has been shown that complex hand movements activate very specific brain areas [62, 63, 64], though some research highlighted the importance of defining a complex hand movement [62, 63]. Thus, given the fact that most studies so far focused on sequential hand manipulations, it might be interesting to specifically inspect fine finger control contrasted with crude power-based gestures. There are multiple ways to approach such an analysis, but as demonstrated in numerous studies (e.g., [66, 67, 36]), the combination of EEG and HDsEMG appears to be a very powerful technique. In the case of fine finger control, it might be therefore useful to inspect EEG waveforms corresponding to different hand gestures and seek any interesting and significant anomalies.

As much as the approach involving simultaneous recordings of EEG and HDsEMG is promising, it requires HDsEMG decomposition, which appears to be a non-trivial task on its own. Despite multiple invented decomposition algorithms (e.g., [8, 28, 9, 10]), many of which report truly outstanding results, none of them are publicly available, which could be due to many reasons. As these methods seem to be crucial for an effective EEG analysis, it might be valuable to explore the real-world challenges of modern HDsEMG decomposition methods. This particular problem links to the research question Q1.

2.4 Goals and Objectives

The purpose of this section is to clearly state what this project aims to achieve (the goals) and through what means (the objectives).

The goals of the project at hand are as follows:

- G1: Investigate and harness HDsEMG decomposition.
- G2: Analyse EEG waveforms obtained during the performance of primal and fine hand movements.

In fact, these are directly linked to the previously discussed research questions (Section 2.3) as the primary purpose of this project is to answer them.

The objectives of this work describe how the goals are going to be accomplished, in the given order. These are as follows:

- O1: Replicate one of the state-of-the-art HDsEMG decomposition methods.
- O2: Evaluate the implementation against simulated HDsEMG signals.
- O3: Decompose real HDsEMG recordings of the two types of hand gestures into underlying sources.
- O4: Track common motor units active across subsequent contractions.
- O5: Build EEG waveforms spike-triggered by the obtained motor unit spike trains.

- O6: Analyse produced EEG action potential shapes.

The first two objectives relate to the goal G1 as they are about having a working HDsEMG decomposition method. The other four show the path to the goal G2, comprising the processing of real HDsEMG recordings, creating EEG waveforms, and finally analysing them.

3 Methodology

This section discusses in detail each aspect of the chosen methodology in order to reach the specified goals and objectives. The core of the approach taken here is the decomposition procedure (Section 3.2), which will process various HDsEMG datasets (Section 3.1). The decomposition results will be further validated through a set of evaluation metrics commonly used in the field (Section 3.3). Furthermore, for the purpose of a later EEG analysis, there is a need to track motor units that are common across subsequent contractions but within a single experimental session (Section 3.4). Once all the ingredients are ready, the EEG STAs will be generated (Section 3.5), enabling the final analysis and the end goal of this study. Finally, Section 3.6 gives a summary of how all the developed components work together and create the proposed solution as a whole.

3.1 Data

There are two types of data utilised in this project: simulated and real recordings. The former, described in Section 3.1.1, provides the means of a thorough validation of the replicated decomposition method as it includes the ground truth information that can be compared to the obtained results. The other dataset, which consists of real experimentally collected HDsEMG and EEG recordings (Section 3.1.2), is the subject of the main analysis for this project. More precisely, the HDsEMG part of the data will be decomposed by the replicated method, the results of which will be used to generate the spike-triggered EEG waveforms out of the EEG recordings.

3.1.1 Simulated Data

This dataset serves as a tool to test the implementation of the chosen decomposition algorithm. For a full description of the data, refer to [68]. These artificial HDsEMG signals have been generated according to a specific model [69], and mainly for the purpose of testing decomposition procedures. They include 15 sets of recordings, each lasting for 16 seconds and sampled at 4096 Hz. The data simulate a 9 by 10 single differential electrode grid, resulting in 90 observations overall. In terms of variability, there are three muscle excitation settings being simulated: 10%, 30% and 50% MVC, each repeated five times to generate different recordings. The signals are free from noise. Although there are ways to add noise to the provided data, this step is considered unnecessary in the case of this project as the goal is merely to test the implementation of an existing algorithm, not to develop a new technique. Simply confirming the correctness of the implementation should suffice, without the

need to push the algorithm’s performance to its limits. In addition, the data contain spike trains of the true underlying sources that were used to generate the simulated EMG signals, enabling a thorough assessment of the performance of the decomposition method.

3.1.2 HDsEMG and EEG

This experimental dataset consists of HDsEMG and EEG signals recorded simultaneously while performing two specific hand manipulations by the subjects: a power grip (closed hand, primal movement), and a pinch gesture (index finger touching the thumb, fine control movement), both of which are illustrated on Figure 1. Volunteers were told to try to maintain a constant force level at 10% MVC and had real-time visual feedback throughout each trial. EEG data were collected through 64 channels placed according to the 10-20 international system, sampled at 8192 Hz. In addition, Common Average Referencing (CAR) was applied to the data, followed by a third order Butterworth band-pass filtering with 0.5 and 40 Hz cutoff frequencies, finally downsampled to 4096 Hz. The HDsEMG, on the other hand, was acquired via a 9 by 14 surface electrode grid (126 channels), sampled at 16384 Hz, and placed on the participant’s forearm (anterior part). This data was also referenced (CAR) and 3rd order band-pass filtered but between 20 and 500 Hz, followed by downsampling to 4096 Hz. On top of that, a small number of noisy channels were identified, for both EEG and HDsEMG, per each subject and excluded from further analysis. An example of how HDsEMG channels were inspected is demonstrated in Figure 2.

Five subjects participated in the experiment (2 males, mean age \pm standard deviation = 26.6 ± 3.6 years old), repeating six times each movement type in randomised order, resulting in 12 contractions overall per session. Four subjects performed five sessions, while one of them did only two due to issues with data collection. Some of the recordings had to be discarded due to unacceptable noise levels which were noted during data collection. The MVC level was calibrated for each participant by asking to apply 100% MVC for 10 seconds, followed by 60 seconds of rest (no force level). The scheme was repeated 3 times per each gesture type at randomised order.

Overall, the purpose of these data is to investigate the eventual discrepancies between the aforementioned two hand movements. More precisely, the idea is to decompose HDsEMG and compute EEG ERPs, with the resulting MU spike trains used as triggers.

3.2 Decomposition

This section focuses on the description of the employed decomposition strategy. Although its central part is the identification of underlying sources from given observations (i.e., the decomposition itself), it is imperative to perform some additional steps before and after the algorithm. More precisely, the pre-processing stage helps to maximise the overall performance of the decomposition, while the post-processing phase retains only high-quality results and prepares them for further analysis. In essence, the approach taken here expects its input to be in the form of multiple observations

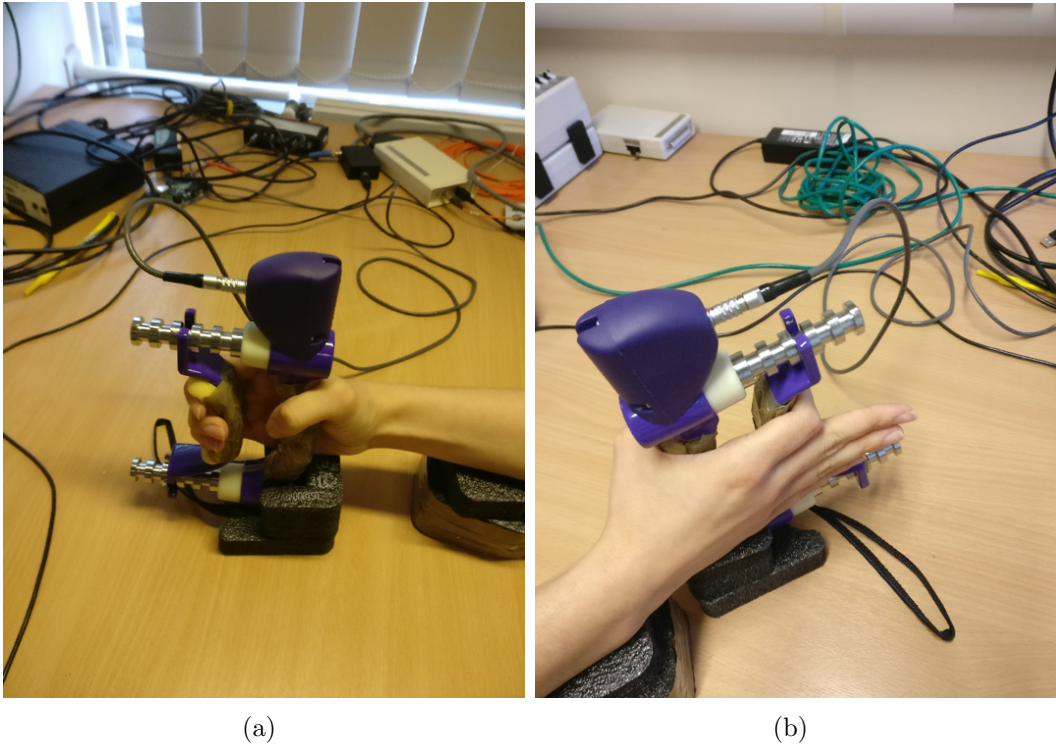


Figure 1: Demonstration of the studied hand movements: (a) power grip, (b) pinch.

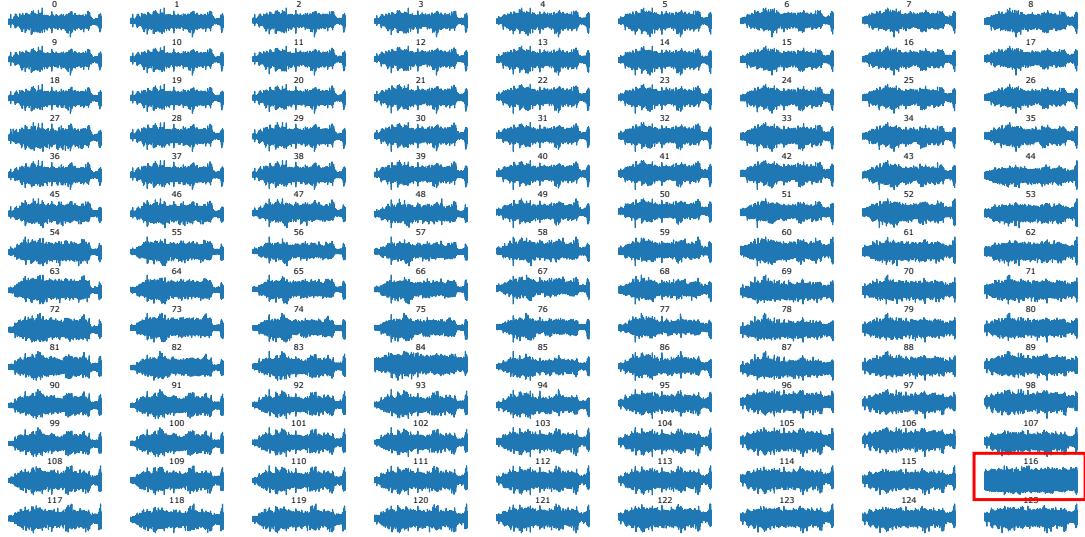
that refer to the electrodes used at the time of data collection. The final result then consists of spike trains of extracted sources. It is worth noting that through this approach the MUAP shapes of retrieved sources are lost as the method focuses exclusively on discharge times, although these waveforms can be easily reconstructed through spike-triggered averaging using the discharge times of the spike trains.

A general overview of the employed strategy to sEMG decomposition is described in Algorithm 1, the components of which are discussed in detail in further sub-sections. A more detailed overview of the decomposition algorithm itself is presented separately (Section 3.2.3) due to its complexity. Each individual pre- and post-processing step is explained in Sections 3.2.2 and 3.2.4 respectively. In addition, for the convenience of the reader, the convolutive data model, which the algorithm is based on, is briefly discussed in Section 3.2.1.

3.2.1 Data Model and CKC

The decomposition algorithm employed as part of this project is based on the convolutive data model and the convolution kernel compensation approach, both of which are briefly described here to aid the understanding of the method and facilitate an in-depth discussion of the procedure later on. For a comprehensive description, refer to [8].

Data Model. The observations $x_i(n)$ are modelled as M time series, each consisting of a mixture of N different symbols (i.e., MUAPs) of length L , where the same symbol is expected to be separated by at least a few samples.



(a)



(b)

Figure 2: Example of a visual inspection of all the data channels by analysing (a) raw signals and (b) their power spectra. As can be seen on both pictures, channel number 116 (marked with a red frame for visualisation purposes) is clearly very noisy and should be removed from further processing.

Pre-Processing

- 1) Extend observations by introducing their K delayed repetitions;
- 2) Whiten extended data;

Decomposition

- 3) Use KmCKC algorithm to decompose pre-processed data into IPTs;

Post-Processing

- 4) Extract MU spike trains from IPTs;
- 5) Discard low-quality sources;
- 6) Filter out duplicated results;
- 7) Align spike trains based on their approximated MUAP time lags;

Algorithm 1: High-level overview of the entire decomposition process, including pre-processing, actual decomposition algorithm, and post-processing. The KmCKC method is described separately in its own designated section due to its complexity.

$$x_i(n) = \sum_{j=1}^N \sum_{l=0}^{L-1} a_{ij}(l) t_j(n-l); \quad i = 1, \dots, M \quad (1)$$

Where a_{ij} denotes the j th symbol observed in the i th channel and t_j is the pulse train corresponding to the repetitions of the j th symbol. Furthermore, under noisy conditions, additive noise $\omega_i(n)$ is also considered, resulting in the following:

$$y_i(n) = x_i(n) + \omega_i(n) \quad (2)$$

For the purpose of the further analysis, it is helpful to transition to the matrix form, by extending the observations $y_i(n)$ by its $K - 1$ delayed repetitions.

$$\bar{y}(n) = [y_1(n), y_1(n-1), \dots, y_1(n-K-1), \dots, y_M(n), \dots, y_M(n-K-1)]^T \quad (3)$$

Applying the same transformation to the noise $\omega_i(n)$, gives the following:

$$\bar{\omega}(n) = A\bar{t}(n) + \bar{\omega}(n) \quad (4)$$

Where A is the mixing matrix and $\bar{t}(n)$ denotes the pulse train extended as follows:

$$\bar{t}(n) = [t_1(n), t_1(n-1), \dots, t_1(n-L-K+2), \dots, t_N(n), \dots, t_N(n-L-K+2)]^T \quad (5)$$

$$A = \begin{bmatrix} A_{11} & \dots & A_{1N} \\ \vdots & \ddots & \vdots \\ A_{M1} & \dots & A_{MN} \end{bmatrix} \quad (6)$$

The mixing matrix then contains the symbols a_{ij} as follows:

$$A_{ij} = \begin{bmatrix} a_{ij}(0) & a_{ij}(1) & \dots & a_{ij}(L-1) & 0 & \dots \\ 0 & a_{ij}(0) & \dots & a_{ij}(L-2) & a_{ij}(L-1) & \dots \\ \vdots & & \ddots & \ddots & \ddots & \ddots \\ 0 & \dots & 0 & a_{ij}(0) & \dots & a_{ij}(L-1) \end{bmatrix} \quad (7)$$

Convolution Kernel Compensation. There are a few crucial assumptions made by the CKC approach. Firstly, the number of observations M is expected to be larger than the number of symbols N . Secondly, the extended pulse trains \bar{t}_j are assumed to be weakly correlated. Lastly, the extension factor K should satisfy the following formula: $KM \geq N(K + L - 1)$ [8]. Then, the activity index, which indicates the existence of at least one source at positive time instants, can be calculated as follows:

$$\gamma(n) = \bar{y}^T(n) C_{\bar{y}\bar{y}}^{-1} \bar{y}(n) \quad (8)$$

Where $C_{\bar{y}\bar{y}}$ is an auto-correlation matrix of the extended observations, computed as per Equation (9).

$$C_{\bar{y}\bar{y}} = E[\bar{y}(n)\bar{y}^T(n)] \quad (9)$$

Next, by using a single time instant, an initial source candidate can be approximated by:

$$t_{n_0}(n) = \bar{y}^T(n_0) C_{\bar{y}\bar{y}}^{-1} \bar{y}(n) \quad (10)$$

Which, as pointed out in [8], can be considered a full source approximation given a large enough set of time instants belonging to a single source:

$$t_{n_0}(n) \approx \bar{t}_j(n) \quad (11)$$

This can be achieved by finding the mean vector given the time instants contributing to a specific source:

$$c_{\bar{y}t_j} = \frac{1}{\text{card}(n_k)} \sum \bar{y}(n_k) \quad (12)$$

Then, the mean vector can be finally used to approximate the entire j th pulse train:

$$\hat{t}_j(n) = c_{\bar{y}t_j}^T C_{\bar{y}\bar{y}}^{-1} \bar{y}(n) \quad (13)$$

As a consequence, the entire problem can be narrowed down to that of identifying a small subset of time instants that likely belong to a specific, ideally single, source. This in turn enables estimating a full IPT.

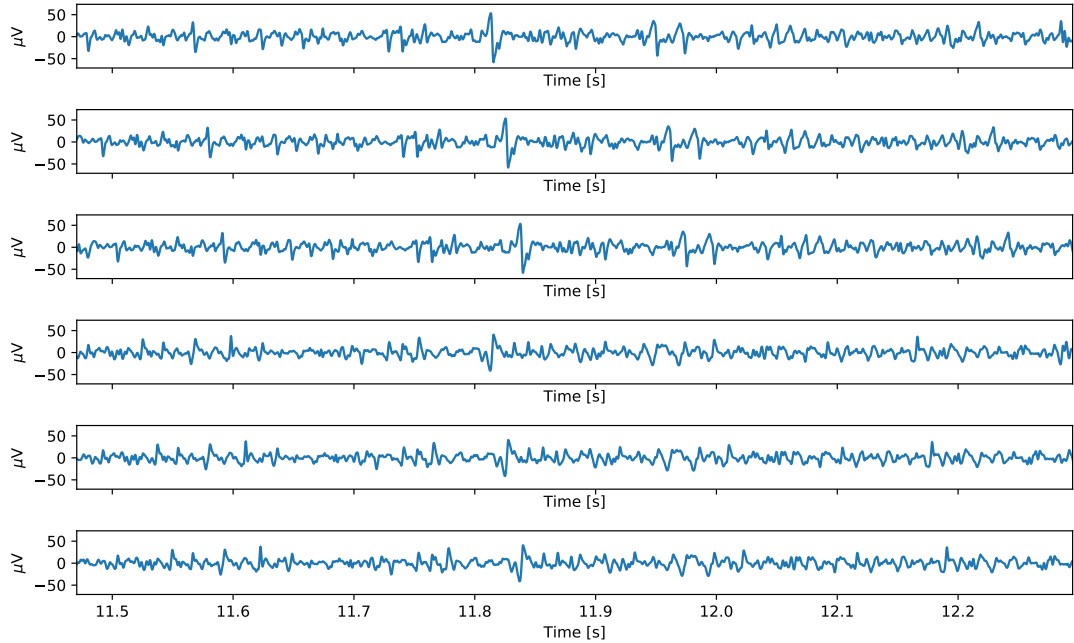


Figure 3: An example of extending given observations by introducing their delayed repetitions. The example demonstrates two channels with their two subsequent repetitions ($K = 3$), resulting in six observations overall. The shift between each consecutive repetition has been increased to 50 for visualisation purposes.

3.2.2 Pre-Processing

Apart from general data pre-processing that involves referencing and filtering, there are two data transformation steps specific to decomposition: a) extending data by a given number of delayed repetitions, and b) whitening. These will be further discussed in the following paragraphs.

Extension Factor. Another pre-processing step, common across many decomposition approaches, involves a so-called extension factor. The idea there is to create artificial observations by introducing delayed repetitions of all original channels, where each consecutive duplicate is shifted forward by one time instant. The extension factor K then specifies how many versions of each channel should exist. For instance, $K = 1$ means no duplicates will be introduced, whereas $K = 2$ will add one delayed copy per each channel. In general, as pointed out in [10], the extended observations help with the inverse of the auto-correlation matrix in the CKC approach (Equations (8), (10) and (13)). An example of the data extension is demonstrated in Figure 3.

Although there is no universal K value generalising to all use cases as it depends on many factors, [10] proposes a formula ($K \geq (N/M)L$) to help find the optimal K for a given problem. In addition, [10] argues that in general increasing K improves the amount of obtained sources, though the authors also point out they observed a plateau at $K = 16$, above which there was little to no improvement. It is also worth noticing that larger K increases data size and hence computational needs of the algorithm, usually resulting in longer decomposition times.

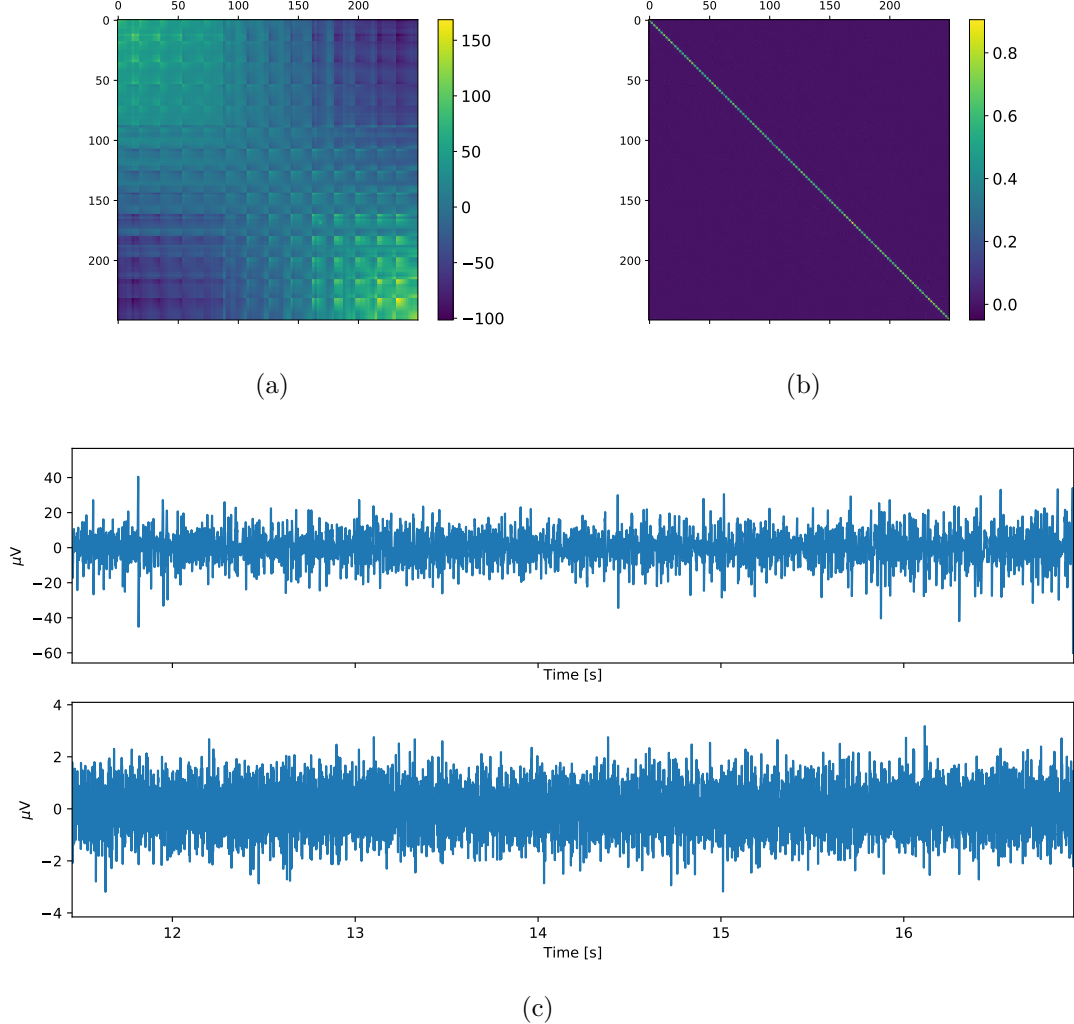


Figure 4: An example of the auto-correlation matrix computed (a) before and (b) after whitening. Subfigure (c) demonstrates a single channel before (top) and after (bottom) whitening.

Whitening. The last pre-processing step is whitening, which specifically aims at reducing the contribution of noise within the data. There are many whitening techniques available, but they almost universally share the requirement of zero-mean data. Thus, as a pre-step to whitening, it is imperative to subtract the mean from all the observations. A specific whitening method often incorporated in EMG decomposition (e.g., [8, 10]) is referred to as convolutive spherling [70]. The whitening approach described here is discussed in more detail in [10]. An example of how whitening affects raw signals and their auto-correlation matrix is depicted in Figure 4.

Given extended observations $\bar{y}(n)$ and the whitening matrix W , the whitened extended observations can be obtained as follows:

$$z(n) = W\bar{y}(n) \quad (14)$$

- 1) From each observation subtract its mean value;
- 2) Compute the auto-correlation matrix $C_{\bar{y}\bar{y}}$ as per Equation (9);
- 3) Perform the eigenvalue decomposition as:
 $d, U = \text{eigenvalue_decomposition}(C_{\bar{y}\bar{y}})$, where d denotes a vector of eigenvalues and U a matrix of normalised eigenvectors;
- 4) Calculate the regularisation factor r as the mean value of the smaller half of the eigenvalues in d ;
- 5) Create the diagonal matrix D as $D = \text{diag}(1/\sqrt{d+r})$;
- 6) Using U from step 3) and D from step 5), obtain the whitening matrix W as $W = UDU^T$;
- 7) Whiten the observations $\bar{y}(n)$ as $z(n) = W\bar{y}(n)$, as per Equation (14);

Algorithm 2: A pseudocode of step-by-step instructions of how whitening can be applied to given observations.

Then, the whitening matrix is defined as:

$$W = U D_S^\gamma U^T, \text{ where } \gamma = -1/2 \quad (15)$$

Next, assuming the whitened extended observations $z(n)$ have an auto-correlation matrix corresponding to the identity at zero time lag, it can be written as:

$$C_{\bar{y}\bar{y}} = U D_S U^T \quad (16)$$

Where the auto-correlation matrix $C_{\bar{y}\bar{y}}$ is given as per Equation (9). The diagonalisation matrix U can be obtained through eigenvalue decomposition, with regularisation factor set to the mean of the smaller half of the eigenvalues of the auto-correlation matrix $C_{\bar{y}\bar{y}}$ [10]. For a detailed list of instructions see Algorithm 2.

3.2.3 KmCKC

The decomposition approach taken in this project employs the K-means CKC algorithm. It is based on the same principles, described in Section 3.2.1, as other CKC-based methods. Despite its roots, there are also some major discrepancies when compared to the classic CKC. Firstly, it uses a different strategy to find the set of candidate time instants belonging to one source, which is accomplished by utilising the K-means clustering technique. Secondly, KmCKC introduces a refinement procedure that improves the quality of approximated sources. As any other variation of CKC, the method assumes some data pre-processing performed beforehand that helps to deal with noisy signals. In terms of the raw outputs, they are in the form of IPTs, which are rarely useful in this representation and hence have to be post-processed as well. A detailed list of steps of the algorithm is presented in Algorithm 3.

The first three steps of the method are shared among most of the CKC-based approaches. Their goal is to find the initial vector using the starting point selected from the computed activity index. The following fourth step is to select the time instant

- 1) Compute the activity index γ (Equation (8));
- 2) Find the starting point as $n_0 = \underset{arg}{median}(\gamma)$;
- 3) Using (10) and n_0 , find the initial vector v_{n0} ;
- 4) Find the highest peak in v_{n0} and denote its time instant as n_1 ;
- 5) Approximate the vector v_{n1} using (10) and n_1 ;
- 6) Identify 30-60 highest peaks in v_{n1} and denote their time instants as φ_{nc} ;
- 7) Take the values from all observations corresponding to φ_{nc} and feed them to the K-means clustering procedure with two clusters;
- 8) Store the time indexes of the larger cluster as φ_{nv} ;
- 9) Using φ_{nv} and Equations (12) and (13), estimate the entire jth pulse train;
- 10) Store the time instants of the r highest peaks in the estimated pulse train as φ_{nu} ;
- 11) Using φ_{nu} and Equations (12) and (13), estimate an improved jth pulse train;
- 12) Increment r by N_p ($r = r + N_p$);
- 13) Repeat steps 10-12 h times;
- 14) Set activity index γ to zero for all time instants φ_{nv} ;
- 15) Repeat steps 2-14 N_{mdl} times;

Algorithm 3: Pseudocode of the KmCKC decomposition algorithm.

corresponding to the highest peak found in the previously computed vector, which in turn is used to calculate a second vector. This is the first difference from the classic CKC approach, which selects a random peak instead. Next, the times of a subset of the highest peaks found in the second vector are clustered into two groups based on their values from the actual observations. The reason behind this step is that the group representing a single source will be larger in terms of the number of entries, which is indeed in line with step (8). This method of separating sources from each other is radically different from the classic CKC, which instead attempts an exhaustive search within all the pairs of approximated vectors. In step (9), the group of spike times with the largest peaks is used to approximate the entire pulse train. This is where many algorithms proceed to the next iteration of the main loop in order to find the next source. However, KmCKC attempts to improve the candidate by selecting an increasingly large number of the highest peaks from repeatedly reconstructed sources. This refinement procedure is justified on the ground that the highest peaks that are repeatedly selected across the iterations become more prominent while the smaller ones, which likely belong to a different source, shrink. Finally, the algorithm ends with a common step of updating the activity index to reduce the probability of selecting the same source again. This entire procedure is repeated a fixed amount of times, which should be large enough to identify as many sources as possible, but also practically small enough as past a certain plateau point there is usually no further improvement.

One of the advantages of the KmCKC algorithm is that its official description, as presented by its authors in [9], is relatively easy to understand and accurate enough to be replicated without worrying about any unspoken algorithm constraints that would

limit its code implementation in practice. This is in contrast to vanilla CKC, which cannot be easily implemented if its official algorithm specification, as provided in [8], is taken literally to write the code. This is because a CKC implementation that exactly matches the pseudocode provided in [8] is unacceptably slow and hence impractical, mostly due to performing an exhaustive search in the middle, which in practice often results in around 24 million iterations (combinatorial explosion). Apparently, there are ways to address this by imposing some extra constraints on the algorithm, but they are not mentioned at all in the official publication that introduced CKC ([8]). That is why KmCKC is considered advantageous in this matter as it is more accessible for replication purposes than CKC.

Moreover, due to the clustering part, KmCKC can be relatively fast, although it highly depends on chosen parameters controlling the number of iterations performed. Furthermore, according to a recent study on the best practices in sEMG decomposition [17], BSS methods are not fully automated as some manual steps based on the observation of intermittent results are recommended in order to reach the optimal performance. However, KmCKC seems to be attempting to automatically perform the improvements that otherwise need to be handled manually. More concretely, this is achieved by the refinement loop towards the end of the procedure.

With regards to the negative side of the KmCKC approach, perhaps its biggest drawback is its lack of determinism, most likely due to the random aspect of K-means clustering. To counteract this unwanted behaviour, the method can be used multiple times on the same dataset to increase the consistency of the results, though this tactic will inevitably increase the overall running time. K-means clustering is also known to suffer from getting stuck in local minima [71], giving yet another reason to run the decomposition process more than once on a given data.

The algorithm requires a set of parameters that can be modified to suit the problem at hand. Although the authors of the method do not provide universal values that would work for all datasets, there is usually a good default number for each parameter that can be considered a good starting point. Firstly, the number of iterations in the main loop, referred to as N_{mdl} , controls the number of candidate sources the method produces. The higher the value of the parameter, the higher percentage of the results are duplicated. On the other hand, more iterations are likely to deliver a higher amount of unique sources. In the case of real, noisy experimental recordings, a value of 350 seems to be a reliable default, at least for the number of electrodes and the extension factor used in this study (126 and 16 respectively). Furthermore, there is a set of three parameters controlling the refinement phase: r , N_p and h . The first two control the number of the highest peaks selected, starting number and increment value respectively. The last one is the iteration count. The optimal values may again depend on the level of noise involved, but the defaults consisting of $r = 5$, $N_p = 5$ and $h = 40$ are usually the best starting point. Moreover, the number of clusters used in K-means can be increased to higher values than two, though operating on exactly two groups usually gives the most stable results. Another parameter is the amount of highest peaks selected for further processing by the clustering procedure (step 6) in the Algorithm 3). According to the performed empirical tests, a value of

60 produces the most stable results. Finally, as already mentioned, the method is not fully deterministic, which can be tackled by multiple runs on the same data. For our considered use case, executing the algorithm five times and pooling the results of the five runs seems to be a reasonable trade-off between running time and consistency of the results.

3.2.4 Post-Processing

The raw outputs of decomposition algorithms are rarely of much use instantly without any further processing, mostly due to them being in the form of IPTs, but also because they can be duplicated or of low-quality. Thus, a set of reliable post-processing steps are crucial in order to make decomposition outputs useful for any further analysis, though establishing them is not a trivial task as the literature is a bit vague in this matter, despite their importance. There are three post-processing steps that are considered critical for sEMG decomposition: a) extracting spike trains from IPTs, b) discarding low quality sources, and c) removing duplicated results. There is an optional fourth step which depends on how the results are to be used in further analyses. This additional action involves re-aligning the resulting spike trains to ensure the triggering event happens at the centre of the channel's window in terms of time. All four steps are discussed in detail in the following paragraphs.

From IPTs to Spike Trains. The first step involves extracting peaks from IPTs. Each IPT is supposed to contain only one underlying source, hence the highest peaks are expected to form a spike train of one motor unit. In other words, the goal is to store the time indexes at which the selected peaks happened, which then can be easily transformed into an array of 0s and 1s, where 1s refer to those time instants containing peaks.

As the raw algorithm output is not of much use without further transformation, the exact procedure of such conversion is of high importance, especially since different conversion strategies can result in different outcomes, that is, spike trains. Unfortunately, this aspect is neglected in the literature, occasionally briefly described, and skipped entirely most of the time.

One specific recommendation on that topic is provided in [10], suggesting to square the output first, feed all detected peaks into K-means clustering with two clusters, and choose those spikes that belong to the higher centroid. A clear advantage of this approach is the lack of any arbitrary thresholds. On the other hand, it is most reliable when the distance between the two clusters is high enough to be certain they are clearly different. This is where the silhouette score (SIL) comes handy as it is a measure of the distance between given clusters. A score of at least 0.9, as suggested by [10], is supposed to guarantee satisfactory separation. However, the problem with this approach is the fact that it is highly difficult in practice to obtain sources meeting the criteria of SIL score above 0.9 and other quality metrics, such as coefficient of variation (which will be discussed below), at the same time. Relaxing the SIL threshold to lower values makes it more feasible to meet other requirements, but then the between-cluster distance is smaller, resulting in the output spike train containing an unacceptable level of noisy peaks. Thus, this conversion methodology

turns out to be overly strict in practice, rendering it unsuitable for this project.

The other approach, involves a dynamic threshold applied to squared IPTs [12]. The reasoning behind this idea is that different sources can vary in terms of the level of noise they contain and hence finding a universal threshold for all use cases might be suboptimal. This is why the authors propose to search for the best threshold, on a source-by-source basis, by optimising the Pulse-to-Noise Ratio (PNR) [72] metric. As much as this approach looks appealing and sensible on the surface, it does not lead to meaningful results without reasonable stopping criteria, which is, unfortunately, not discussed by the authors. Blindly optimising this metric may simply lead to increasingly higher thresholds and very few spikes making it to the end as a result. As spike trains with less than 10 peaks are of little use for the purposes of this project (and meaningless from a physiological perspective), this conversion strategy appears to be requiring more work before incorporating it into practical problems.

Given the above discussion and discovered issues with the proposed methods, it is not particularly clear what is the best approach to transform IPTs into spike trains, although at least most of the recommendations agree on squaring the result first before proceeding. This indeed seems reasonable as it presumably amplifies higher spikes and shrinks those closer to zero. With regards to the peak detection, it is fairly common within the spike sorting community to use a threshold based on the standard deviation of the signal, usually within a range of 2.25 and 3.5 [73]. There are also more robust thresholds, based on the signal's median [74], though it seems to be more applicable in the realm of invasive recordings, where the amplitudes of the spikes are much higher than those from surface EMG signals. According to the experiments conducted as part of this project, a threshold of exactly three standard deviations of the squared signal proved to be the most reliable across various datasets. An example of this specific strategy is demonstrated on Figure 5.

Quality Filter. Even though there is no ground truth to evaluate the quality of the decomposition in most real-world decomposition problems, there are still ways to ensure the obtained results are meaningful from a physiological perspective, and of relatively good quality to some degree. The goal here is to incorporate some commonly used metrics and define certain thresholds for each of them. Any reconstructed source not meeting defined criteria is then discarded from further analysis.

One of the assumptions about muscle innervation is that motoneurons fire in a relatively consistent rhythm, at least under stationary conditions allowing for excluding muscle fatigue. As a result, the Inter-Spike Intervals (ISI) of the obtained MU spike trains are expected to be fairly regular as well. More concretely, the Coefficient of Variation (CoV) of those intervals should be below a certain percentage (see Equation (21) for CoV_{ISI} calculation). The actual threshold may depend on the MVC involved in the study, but as demonstrated in [10], CoV_{ISI} should be anticipated to be below 30% for movements involving 10% MVC and below 50% for higher MVC values. In fact, CoV_{ISI} of 30% has been shown to correspond to decomposition accuracy of 90% [75]. Moreover, it is standard practice to disregard abnormally short ($< 25\text{ms}$) or long ($> 250 \text{ ms}$) intervals from CoV_{ISI} calculations [10], thus allowing for some decomposition inaccuracies (false positives) and scattered groups of regular

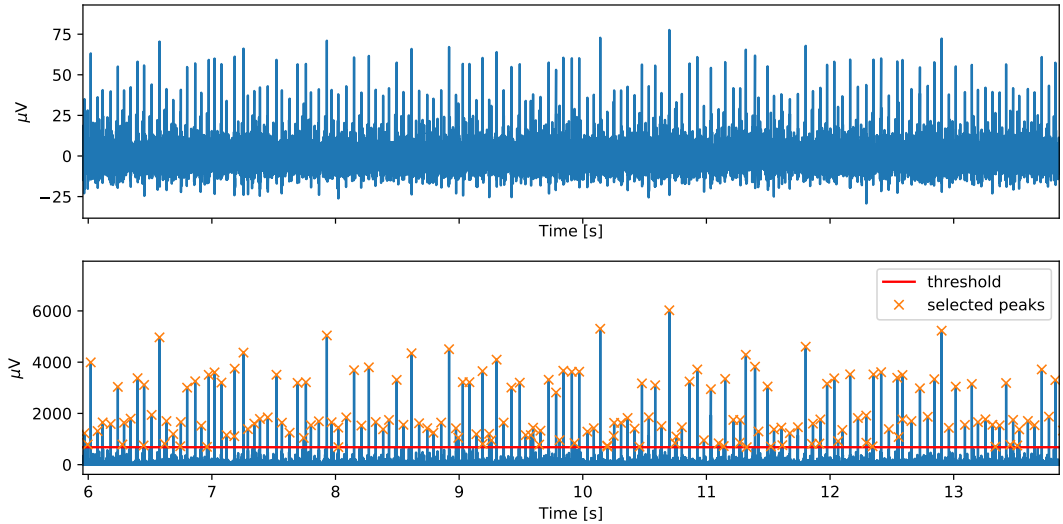


Figure 5: A demonstration of the employed spike train extraction approach. The top plot shows a raw decomposition result in the form of the IPT signal. The bottom one presents the same IPT but squared, together with the peak threshold set to three standard deviations (red line), and selected spikes (orange crosses).

spikes.

The regularity of spikes is certainly important, but so is their frequency of firing, often measured in pulses per second, and aggregated into the Mean Discharge Rate (MDR) averaged over an entire data example. The exact range of sensible MDR values may depend on the physiological properties of studied muscles, but it is usually defined as [6, 40] [10]. Thus, any source having the MDR outside of the agreed range should be excluded from further analysis. It is also worth noting that some studies use a slightly simpler metric that focuses on a minimum number of detected spikes in a given train. For instance, [17] suggests a number of 10. However, a simple value defined in this way loses its meaning if the length of the recordings varies across experiments. In fact, any carefully defined MDR range should discard overly sparse sources nevertheless.

Another quality filter some studies incorporate is the aforementioned silhouette score, which the method proposed in [10] is heavily based on. However, as discussed above, it is difficult to obtain sources with SIL of at least 0.9 and other metrics at the same time. More specifically, according to experiments performed in this study, obtained sources almost never satisfied both SIL (> 0.9) and $CoV_{ISI} (< 30\%)$ requirements at the same time. Thus, a decision was made to drop the SIL requirement in favour of keeping the CoV_{ISI} due to the latter being considered more important as it ensures low enough variability of spikes, which is expected from a physiological perspective, whereas the SIL score is merely a tool to confidently select peaks from IPTs.

Duplication Filter. Once low-quality results are discarded, the next step is to remove duplicated sources. There are two main reasons why the same source may be discovered more than once. First and foremost, this happens due to the way the CKC-based algorithms are designed. They simply converge to similar results multiple times over the course of entire decomposition. Secondly, there is a chance of discovering a de-

layed version of an already identified source due to the use of the extension factor, as more repetitions of the same data are being decomposed. This problem of finding delayed versions of the same source highlights the importance of comparing obtained results at different time lags.

Grouping the obtained results into similar sources is clearly important as it affects the number of final results, especially if such a number is one of the metrics an algorithm is trying to optimise. However, despite its seemingly obvious importance, no published decomposition method explains any specifics of performing this sort of classification, which is deeply concerning and surprising. This is not much of an issue when comparing the results to the ground truth as simply the source with the highest score can be retained in the case of multiple matches, but it becomes problematic when processing experimental recordings.

Given the lack of concrete recommendations provided by the literature, the following similarity metric (see Equation (17)) has been developed for the purpose of this project. It operates directly on spike trains rather than IPTs as the latter include noisy peaks and their overall amplitude, none of which is informative in this context. The only necessary piece of information is whether a spike exists at a given time instant or not.

$$\text{Similarity}(a, b) = \frac{\sum(a \times b)}{\sqrt{\sum a \times \sum b}} \quad (17)$$

The method compares two spike trains (a and b) at a time, where each train is a binary vector with positive values indicating a spike. The similarity score is simply the number of overlapping spikes divided by the square root of the product of the spike counts of each train. The metric strictly penalises not matching spikes, mostly to avoid falsely high scores in the case of comparing two radically different trains but where one of them has an abnormally large amount of false spikes. The returned score is in the range between 0 and 1, with 1 meaning a perfect match. According to performed tests, two spike trains with the similarity score lower than 0.1 can be confidently categorised as different. In addition, due to the possibility of obtaining delayed versions of the same source, it is necessary to check the similarity between two trains at different time lags. In the event of finding two similar sources, the one with the lower CoV_{ISI} value is maintained.

Spike Train Alignment. Due to the fact that it is highly likely to obtain delayed versions of the underlying sources, mostly because of the extension factor, it might be desirable to correct their timings. This step can be considered optional depending on the use case, but it is certainly useful for this particular project as the extracted HD-sEMG spike trains and the EEG signals they are combined with must be synchronised to avoid jitter in the EEG ERPs. Thus, the resulting spike trains are re-aligned. An example of how re-alignment affects the STAs of a given source is demonstrated by Figure 6.

The alignment procedure is performed as follows. First of all, the MUAP shapes for all the HDsEMG channels are reconstructed through spike-triggered averaging (40 ms

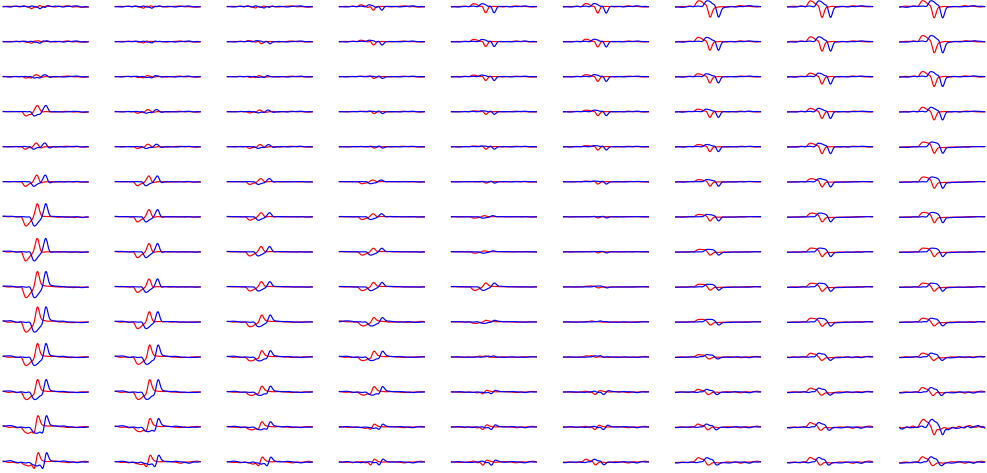


Figure 6: An example result of the spike train alignment. Both MUAPs were estimated through spike-triggered averaging, but using different pulse trains. The red one corresponds to the train before alignment, while the blue one to the corrected one. As a result, the aligned (blue) MUAPs are closer to the center of the averaging windows.

epoch window) using a given spike train. The averages are then squared to account for negative shapes. Next, the channel including the signal with the highest peak value is selected. Then, the time instants corresponding to the peak and the centre of the epoch are compared to each other, resulting in a number describing the time lag between them. The time instants of the spike train in question can then be shifted accordingly by the calculated lag.

3.3 Evaluation

Evaluation is a crucial part of every project as it provides information about the quality of the obtained results. In the case of HDsEMG decomposition, there are a few commonly used metrics, though some of them are only applicable when the ground truth is available. Therefore, the evaluation metrics incorporated as part of this project are divided into two groups: those utilised during the implementation stage when testing against data including a ground truth (Section 3.3.1), and those used at a later stage when assessing the quality of the sources extracted from real recordings (Section 3.3.2).

3.3.1 Implementation Stage

The metrics discussed here assume access to the ground truth and hence cannot be used against true experimental signals. The most commonly used measures of assessment when it comes to decomposition algorithms are *Rate of Agreement* (RoA), *Sensitivity* and *Precision*. Given that a True Positive (TP) characterises correctly identified peaks, a False Negative (FN) the ones that are missed, and a False Positive (FP) those excessive ones that are not present in the gold standard, the three metrics are defined as:

$$RoA = \frac{TP}{TP + FN + FP} \quad (18)$$

$$Sensitivity = \frac{TP}{TP + FN} \quad (19)$$

$$Precision = \frac{TP}{TP + FP} \quad (20)$$

It is worth pointing out that the RoA is somewhat an aggregated version of the other two as it penalises both missed and false peaks at the same time, while sensitivity and precision account for only one of those errors each. Furthermore, when comparing spike trains to each other, a jitter of ± 0.5 ms was allowed, that is, when counting TPs, FNs and FPs. Two sources were considered the same if the RoA was at least 30%. Both aspects are in agreement with the methodologies employed in the literature (e.g., [12]). Apart from those metrics, it is common to report the number of detected sources. Finally, reporting the amount of time the algorithm took to decompose a sample can be informative as well.

3.3.2 Real Recordings

There are two assessment measures chosen to evaluate the results of decomposing real recordings, namely CoV_{ISI} and mean discharge rate. The justification behind both metrics has been already discussed when describing the post-processing steps (Section 3.2.4). The two scores are calculated as follows:

$$CoV_{ISI} = \frac{Std_{ISI}}{Mean_{ISI}} \quad (21)$$

$$MDR = \frac{\#pulses}{signal_duration[s]} \quad (22)$$

When computing CoV_{ISI} all the abnormally short ($< 25ms$) and long ($> 250ms$) intervals were not taken into account [10]. Moreover, according to [75], CoV_{ISI} is strongly correlated with decomposition accuracy. For instance, a CoV_{ISI} of 0.3 corresponds to 90% accuracy. A somewhat indirect evaluation method could also involve the reconstruction and manual inspection of EMG STAs.

3.4 Tracking Common Motor Units

Depending on how the extracted motor units are used in further analysis, and also how the decomposition itself is performed, there might be a need to track those MUs that are active across multiple contractions within the conducted experiment. In this study, each contraction of a given session was decomposed separately, as this approach provides better quality results when compared to decomposing the entire session at once. However, since the ERPs that we are looking for in the EEG signals are of very

small amplitude, the number of spikes used as triggers to calculate the ERPs must be in the order of magnitude of a thousand, which goes beyond the numbers achievable when decomposing individual contractions due to the physiological limitations. Thus, there is a need to identify common MUs across multiple contractions but within a single session so the joint spike trains can be used to obtain accurate EEG ERPs.

There are two major approaches when it comes to motor unit tracking. Some techniques rely on MUAP shapes similarity across channels [76, 77], although the obvious downside is that some characteristics of these waveforms can change over time, for instance, due to muscle fatigue, training or developed pathologies. Other methods attempt to exploit some algorithm-specific intermittent results, such as separation vectors or mixing matrices generated during the decomposition. The latter is usually a byproduct when utilising ICA-based decomposition methods. As discussed in Section 3.2.1, the mixing matrix contains information about different MU symbols and how they relate to involved observations, which in turn can be exploited to identify common sources. This idea was explored in [78], providing a reliable method of tracking motor units given the extracted mixing matrix. The separation vectors, on the other hand, are common for CKC-based algorithms, also called as mean vectors, as provided in Equation (12) (Section 3.2.1). These vectors are in fact linear filters that include information about each observation’s contribution with respect to each approximated source. The downside of relying on those vectors when tracking MUs is that changing the position of the electrode grid will also result in different vectors. Fortunately, this is not a problem for this study as the grid was not removed between experimental sessions of the same subject.

One of the studies utilising separation vectors for this purpose compares them through normalised cross-correlation [79], where the pairs of vectors exceeding a given similarity threshold are categorised as the same. A clear disadvantage of this approach is the use of an arbitrary threshold that may not generalise to other use cases, and which is not properly justified by the authors. The other approach performs a statistical analysis of independent components [80], which in fact originates from [78] that operates on mixing matrices. The authors offer thorough statistical derivations to ensure the reliability of the procedure. In addition, there is no fixed similarity threshold involved as a parameter, only the desired confidence interval that the results will adhere to. Due to its statistical assurances and suitability to use with separation vectors, this method has been incorporated into this study to track common motor units.

However, at first, the chosen method was not fully compatible with the outputs obtained from KmCKC decomposition. This is because the separation vector associated with a given source in this case is a mixture of delayed versions of smaller separation vectors, which is a direct consequence of the extension factor K that introduces delayed copies of each channel’s observations. As the entries in the separation vectors relate to all the observations incorporated into decomposition, even those artificially created, the vectors include the contribution of the delayed versions of the channels as well. Unfortunately, simply feeding such a complex vector into the tracking method did not work as vectors in this form were too distinct across different sources to be found similar to each other. Deconstructing the vector into its delayed versions and

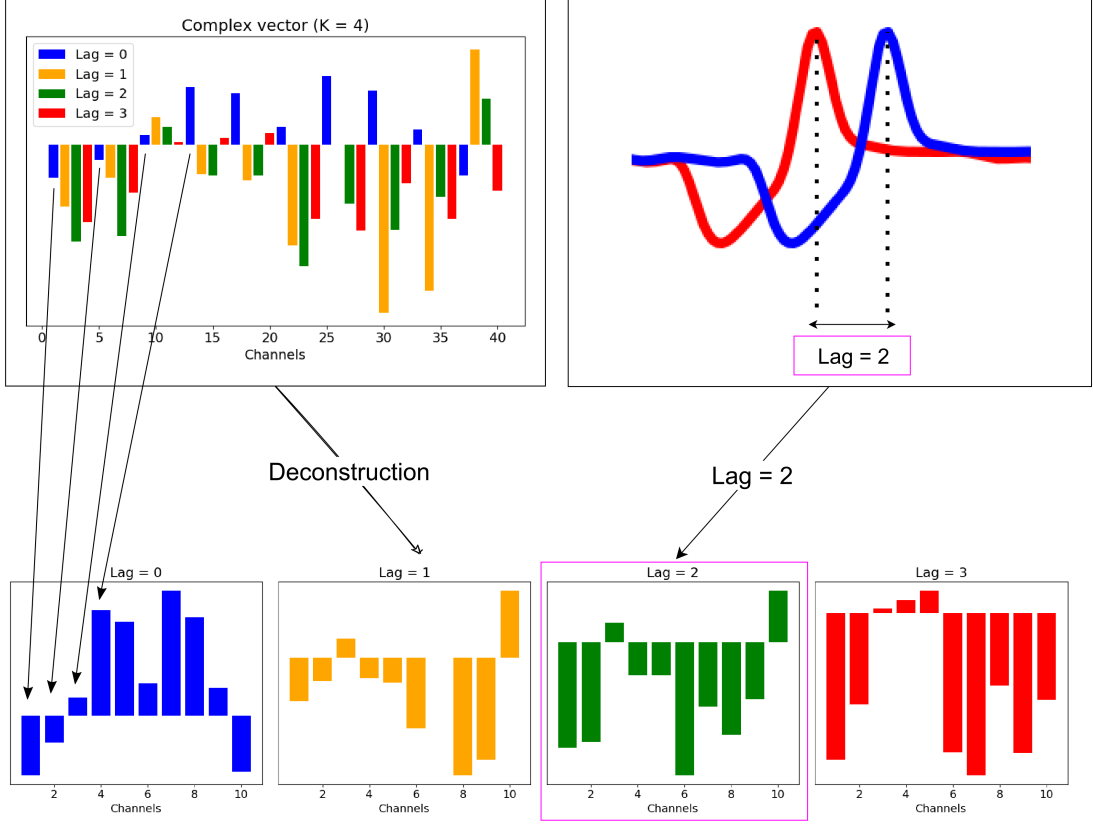


Figure 7: An example of how separation vectors are pre-processed so they can be effectively used in source tracking. Given 10 channels and the extension factor $K=4$, the complex separation vector consists of 40 values (top left), where each of its smaller delayed versions is represented by a different color for illustration purposes. The complex vector is then deconstructed into 4 vectors of size 10 (bottom part). Given the calculated time lag of 2 from the spike train alignment stage of the decomposition post-processing (top right), the most suitable delayed vector is the one corresponding to the lag of 2 (purple box). This selected vector is then used in MU tracking procedure.

passing all of them at once slightly improved the situation, but then the tracking results were full of false positives as the chosen method was not designed to handle different time lags of the independent components. Thus, there was a need to select only one of the delayed versions of the vector that is the closest to the estimated source and then use only that vector for tracking purposes. This was done as follows.

Given the extension factor K , the complex vector (i.e., mixture of delayed vectors) is deconstructed into K individual vectors, each of which is of size matching the original number of channels and is a delayed version shifted in time. For instance, given 10 channels and $K = 4$, the complex vector of size 40 is deconstructed into 4 vectors of size 10. Then, based on the time lag obtained from the spike train alignment (see Section 3.2.4), the vector closest to that lag is chosen over the others. All the complex vectors extracted from a given experimental session are pre-processed in such a way and then finally fed into the tracking procedure. Figure 7 illustrates the process of deconstructing the complex vector into its delayed smaller versions and how the most suitable vector is chosen for further analysis.

3.5 Spike-Triggered EEG Waveforms

This is the very last step of the employed methodology and assumes that both entire decomposition and source tracking have been completed. Since the ultimate goal of this study is to explore differences in the EEG waveforms using spike trains from different hand movement types, three kinds of extracted motor units were incorporated into generating EEG ERPs. These are: a) MUs active at the time of performing the pinch gesture only, b) those present exclusively during the power grip, and c) the sources present in both hand manipulations. Furthermore, as the motor cortex is the brain area of interest in this study, for the following EEG channels the aforementioned ERPs will be generated: FC5, FC3, C5, C3, CP5, CP3 (right hand, left hemisphere), and FC6, FC4, C6, C4, CP6, CP4 (left hand, right hemisphere), all according to the 10–20 EEG system.

In terms of the actual technicalities of computing the ERPs, each individual peak of a given spike train is treated as a trigger, or an event, when selecting EEG epochs. The end result is then the mean signal averaged over all selected epochs, separately per each EEG channel. As the cortical signals are expected to precede the events happening in the muscles, more emphasis should be given to the time period before the triggers. Thus, the goal is to select the epochs that last 1.2 seconds, starting 1.0 second before each triggering spike and ending 0.2 seconds after. The first 200 ms of the epochs (i.e., $[-1, -0.8]$) is then used to apply the baseline correction, that is, the mean of the first 200 ms of each epoch is subtracted from that epoch.

Furthermore, since we are expecting a very localised ERP, we also explored whether the use of a spatial Laplacian filter would help reduce noise in the signal by subtracting the mean of neighbouring EEG channels for each epoch, before averaging over all the results. Such a transformation can potentially remove any similarities across closely-located channels, emphasising the differences as a consequence.

Finally, as a measure of confidence added to the analysis, each averaged waveform should be accompanied by its standard error. Given a vector of measurements x , the error can be calculated as follows:

$$\text{StandardError}(x) = \frac{\text{Std}(x)}{\sqrt{\text{Size}(x)}} \quad (23)$$

Where Size denotes the amount of entries within x (i.e., the number of epochs extracted).

3.6 Overview and Parameters

To summarise all the described components employed in this methodology, together with all the necessary parameters, a diagram presented in Figure 8 shows the entire pipeline of the designed approach.

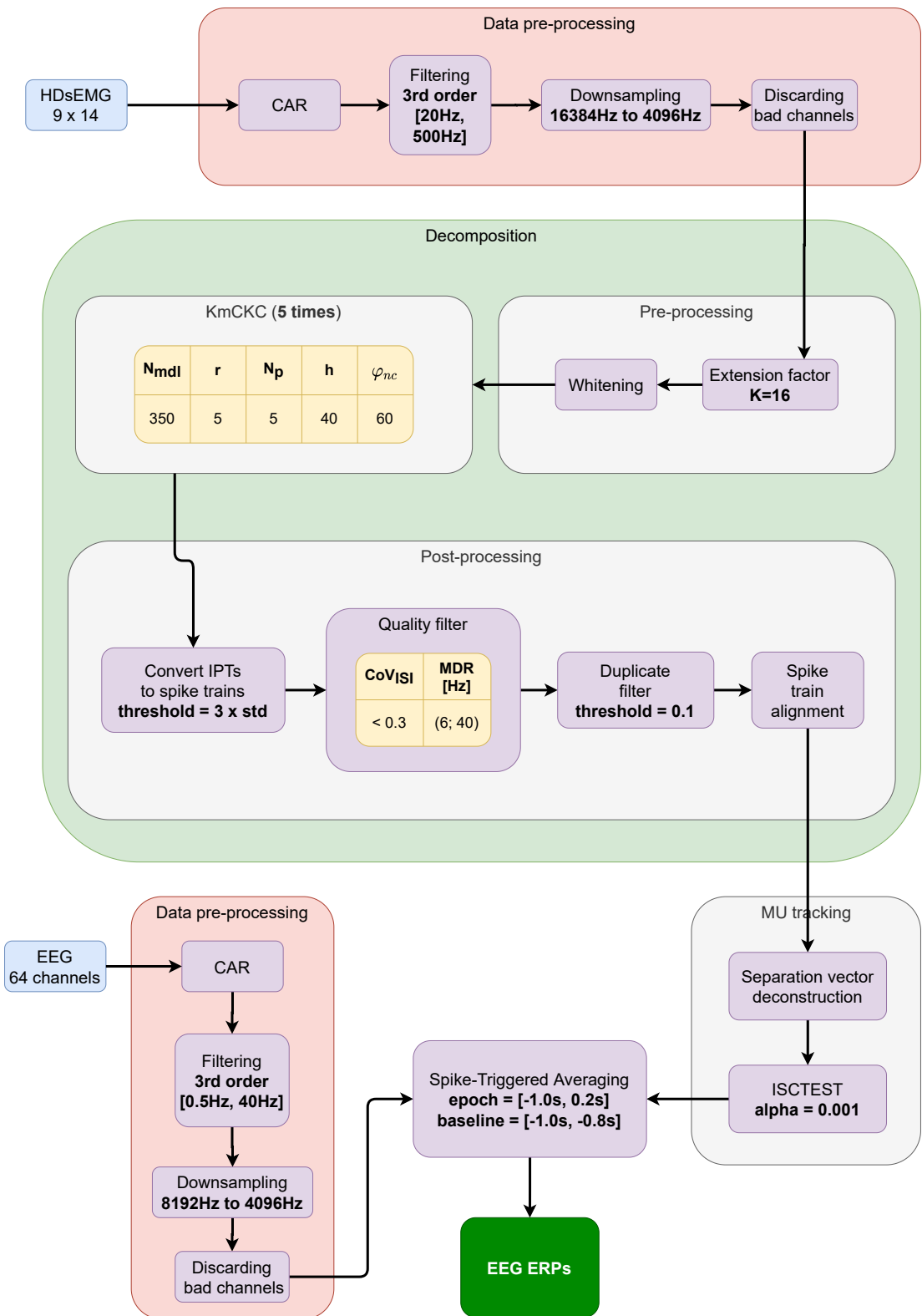


Figure 8: A diagram showing how all the involved components fit together, highlighting all important parameters used.

4 Implementation of KmCKC algorithm

This section discusses the implementation of all the necessary components employed as part of the chosen methodology, described in Section 3. The core components are: a) the KmCKC decomposition algorithm, b) pre- and post-processing done as part of the overall decomposition process, c) MU tracking, and d) EEG STAs. The vanilla CKC method has also been replicated, but due to it showing worse performance than KmCKC it was not used in further analysis. Furthermore, apart from the principal modules, the implementation process was supported by helper scripts developed along the way that facilitated evaluation and debugging, provided useful visualisations, enabled efficient experiments, and helped to find optimal parameters.

In terms of incorporated technologies, the scripts have been programmed in *Python 3*, and built on top of *SciPy* [81], *NumPy* [82] and *scikit-learn* [83] packages. Most of the visualisations have been achieved thanks to *matplotlib* [84], though the ones related to EEG signals were accomplished through the *MNE* package [85]. Lastly, the core of the MU tracking procedure is based on the *ISCTEST* method [80], though it required some additional pre- and post-processing steps to develop a full tracking procedure for the purpose of this project.

When it comes to evaluating all the components of the employed methodology, a few testing strategies were incorporated, depending on their applicability. A preferable way of asserting any software is unit testing as it gives a clear answer whether a given piece of code returns expected results or not. However, such a low-level checking is only feasible for deterministic functions of limited complexity. While some unit tests have been written as part of this project for relatively simple functions, it was certainly not applicable for more complicated modules, such as decomposition or MU tracking. In order to provide at least some level of validation for these complex components, their final and intermittent results were manually inspected and visualised wherever possible. With regards to decomposition algorithms, the usual way of validating them is to decompose simulated data accompanied by ground truth records. In this way, a set of specific evaluation metrics can be used to assess the quality of the produced outcomes. This technique was employed in this project as well, which is further discussed in Section 4.3.

Further subsections discuss some of the challenges encountered when implementing the decomposition parts (Section 4.1), but also present a few experimental modifications tried during the implementation process (Section 4.2). The replication of the KmCKC algorithm is then validated in Section 4.3. The section is concluded with a general discussion about the implementation stage of the project (Section 4.4).

4.1 Challenges

Many challenges have been encountered while implementing the major components of the employed methodology. Most of them were related to the entire decomposition process, comprising the replication of the decomposition algorithm itself, but also all the additional steps required before and after applying the method. In addition, figuring out the MU tracking procedure was also a source of a few issues. All these

are discussed in more detail in the following paragraphs.

Decomposition Algorithm. Most of the issues related to the replication of decomposition methods are generally due to inaccurate or incomplete descriptions when said techniques are introduced in the literature. Firstly, the instructions themselves are often vague as they at times recommend to perform a certain action, but without giving the specifics of how to actually achieve that (e.g., “remove duplicates”). If by any chance such an explanation is given, it, unfortunately, likely misses important details, resulting in a situation where a specific action can be accomplished in multiple ways, possibly introducing unwanted discrepancies in the implementation.

Secondly, the descriptions often lack a thorough explanation of the introduced parameters and constants. This is indeed a problem as very specific parameter values rarely generalise to other recordings. Thus, it is very difficult to find optimal numbers for the problem at hand, further complicated by the lack of a ground truth inherent in these problems. This situation is sometimes improved when a range of acceptable values is given, although without such descriptions, choosing a satisfactory value for a particular case remains problematic nevertheless.

Thirdly, the theoretical derivations that are part of algorithms’ descriptions are at times unfeasible in practice if just taken as they are described. This would not be an issue if such instructions were supplemented with additional notes regarding their practicality. Unfortunately, this is not the case. A concrete example is the provided pseudocode of the classic CKC algorithm, which suffers from combinatorial explosion if taken literally without certain, regrettably not mentioned, constraints.

Another issue is the inconsistency of used evaluation metrics across studies, which in turn makes it difficult to compare proposed methods to each other. Moreover, it is not always clear how exactly the performance scores are calculated, specifically how to count matching pulses when comparing a pair of spike trains. This is non-trivial as frequency sampling affects the precision of obtained spikes, not to mention the possibility of getting delayed versions of actual sources.

There is also a set of problems not necessarily connected to algorithms’ descriptions. For instance, the datasets used for evaluation purposes by other studies are almost never publicly available, seriously hampering the replication process. Likewise, open implementations of proposed methods are scarce and uncommon, eliminating the opportunity to compare a replicated method to its original code. Finally, it has been noticed that some decomposition methods are misleadingly labelled as fully automated, while the experts in the field openly admit that currently available procedures in fact require some manual steps if the accuracy of decomposition results are of high importance. Such overly optimistic statements can create unrealistic expectations and certainly be a source of confusion when either replicating or using said methods.

Pre-Processing. Perhaps the most prominent issue when it comes to decomposition pre-processing is that not all studies devote enough attention to their explanation, even though most works rely on at least some preliminary steps. As a result, the overall pre-processing advice is scattered across literature, lacking universal recommendations within the field. Probably the most common preliminary steps that most studies

seem to agree on are the extension factor and whitening. The issue with the latter, however, is that it is a rather complicated procedure, which seems to be trivialised in the literature. As a consequence, the descriptions often lack important details that leave certain aspects to the reader's interpretation or familiarity with the topic.

Post-Processing. There are three quite problematic issues with regards to decomposition post-processing: a) peak selection, b) removal of duplicates, and c) quality filtering of the sources. Extracting spikes from IPTs is central to decomposition as the raw outputs (IPTs) are of little use in further analyses. Furthermore, various peak selection techniques may result in different spike trains, affecting the overall performance of the algorithm. Despite this fact, the actual strategy of obtaining spike trains is rarely explained. Although there seems to be a relative consensus that IPTs should be squared first due to its clear benefits, there is very little information about how exactly the peaks should be selected afterwards. An intuitive solution is to apply a threshold, above which the pulses are classified as valid, though the choice of the threshold is a non-trivial task. Some methods propose to use clustering to extract appropriate peaks, but it requires very clean results in order to work reliably, something extremely difficult to achieve when decomposing real experimental recordings.

In terms of removing duplicated sources, it directly affects the number of obtained results as in principle the amount of raw outcomes is controlled by the iterations count of the main loop. Moreover, said duplicates are usually not quite the same due to small differences between spikes (e.g., time lags, missed spikes). It is therefore clear that a solid duplication removal scheme is of vital importance, especially since the number of reconstructed sources is often one of the metrics optimised by the algorithms (the more the better). Given the highlighted importance it is particularly surprising that this part of decomposition is universally and completely omitted in the literature. As aforementioned, the differences between spike trains can be subtle, so simply comparing peak positions seems rather naive. It is also worth noticing that this aspect does not constitute a problem when the expected results are known in advance, which is the case with artificially generated data, but it becomes an issue when processing real recordings.

Discarding low-quality sources can also be a source of problems when seeking advice in the literature. This particular step is usually omitted entirely when a new method is introduced, though some specifics are given when algorithms are being applied to a real-world scenario. The only downside is that the details of incorporated quality metrics can differ across studies, making it again difficult to accurately replicate the given method. On the other hand, those differences are understandable to some extent as they depend on the physiological properties of investigated muscles.

All three discussed aspects are considered critical for a correct assessment of any decomposition algorithm and thus it is deeply concerning they do not receive adequate attention in the literature. In the light of unavailable open implementations of the methods, this is regarded as unacceptable as it seriously impacts the replication process, a fundamental aspect of science.

4.2 Experimental Modifications

Apart from replicating the major components as advised by provided instructions, a few custom modifications have been tried in the hope of improving the performance even further. Unfortunately, none of them turned out to be significant enough to keep it permanently. Nevertheless, each attempt is briefly discussed in the following paragraphs for reporting purposes.

Classic CKC and the Refinement Loop. The refinement step introduced as part of KmCKC clearly improves initially approximated IPTs. Thus, it was interesting to investigate how adding such an additional step would improve the vanilla CKC algorithm, without the K-means part. In terms of the number and quality of the extracted sources, the results on average were indeed very similar to KmCKC, proving the usefulness of the added step. However, this modification considerably increased the time complexity of the method to the extent where it was multiple times slower than KmCKC. Given similar results to KmCKC and much slower runtime, this alteration was ultimately abandoned, though at least showed the power of the refinement step.

KmCKC with Additional Refinement. Another improvement loop, in principle similar to that of KmCKC, was also proposed in [10]. Its major differences are that it selects peaks through clustering and optimises CoV_{ISI} metric (the lower the better). Thus, it was of interest to investigate its impact on KmCKC, added on top of its existing refinement step. Unfortunately, the results obtained from such a modified method were similar to vanilla KmCKC at best or even worse, not to mention the additional runtime burden. This perhaps shows there are practical limits of blindly applying refinement iterations, which beyond a certain point can only worsen the obtained sources.

Activity Index Update. There is a common step among CKC-based methods towards the end of the main loop to set the activity index to zero at certain time instants (step 14 in Algorithm 3). Given that most of the decomposition methods are demonstrated to operate on signals sampled at 1024 Hz or 2048 Hz, it was of interest to investigate if setting to zero also the neighbours of said time instants would improve the convergence properties of the algorithm when operating on data sampled at 4096 Hz. According to performed tests, this minor modification can indeed push the method to find a higher amount of unique sources under lower iteration count, which directly translates to a shorter runtime. However, this improvement happened at the cost of general stability of the implementation. Given the risk involved and time constraints of this project, the amendment was reverted, though it might be a fruitful direction for future studies.

Custom Delay Step. The last experimental modification involved using a larger step when extending the recordings by introducing their delayed repetitions. More precisely, the original idea of adding delayed versions of each observation specifies to add each subsequent delayed signal shifted exactly by one data sample. As this project operates on a larger than usual sampling rate for HDsEMG decomposition (4096 Hz), we considered the idea that increasing the shift to larger numbers could positively impact the overall results. Unfortunately, this was not the case as the outcomes were

clearly worse.

4.3 Validation of KmCKC Implementation

The implementation of the KmCKC algorithm was validated against simulated HD-sEMG data, described in Section 3.1.1. Just to clarify, the purpose of the validation was purely to ensure the replication is accurate. There was no desire to push the state-of-the-art of the decomposition as the goal was to replicate an existing method, not to develop a new one.

In terms of pre-processing, no channels were discarded. The recordings were extended ($K = 16$) and whitened. The KmCKC algorithm was run 5 times on each data sample with the following parameters: $N_{mdt} = 350$, $r = 5$, $N_p = 5$, $h = 40$, $\varphi_{nc} = 60$. With regards to post-processing, the resulting IPTs were squared, of which the peaks exceeding the threshold of 3 standard deviations were used to extract the final spike trains. There was no need to utilise the usual duplication filter here as simply keeping the result with the best RoA score was sufficient in case multiple candidates matched a given gold standard source. All obtained sources had to satisfy the following quality criteria: $CoV_{ISI} < 0.5$, $6 < MDR < 40$ Hz. The spike train alignment step was unnecessary in this case and hence was not performed. Table 1 reports the obtained scores, including source count, and grouped by the MVC level. In addition, Table 2 contains information about the average decomposition time, also aggregated by the level of contraction.

4.4 Discussion

As outlined in Table 1, the number of unique MUs extracted from the data declines significantly as the muscle excitation rises. The biggest drop in source count can be observed between 10% and 30% of MVC (42.12 and 29.48 respectively), whereas changing from 30% to 50% MVC decreases only by 6 units. This negative trend indeed makes sense as a higher muscle force positively correlates with more frequent discharges, as exhibited by MDR values, which, in turn, cause a higher probability of source overlap. A natural consequence of more probable superpositions is thus a higher difficulty of separating the signals into underlying sources. Furthermore, an opposite trend with regards to MVC levels can be noticed when examining the overall accuracy of the results. The RoA score increases markedly between 10% and 30% of MVC, from 0.83 to 0.95, followed by a minor rise of 0.02 for 50% maximal contraction. With respect to the sensitivity and precision scores, the algorithm rarely misses any peaks (high sensitivity) but is prone to including false spikes (lower precision). The latter is clearly the source of lower RoA values as sensitivity is almost perfect. The gap in precision between 10% MVC and the other two could be due to the fact that the activity of motoneurons recruited at lower force contractions is more difficult to distinguish from noise and hence resulting in false spikes. Finally, the CoV_{ISI} values, denoted as CoV in Table 1, are clearly correlated with overall accuracy, that is, more regular trains are more likely to have better RoA score, which is in agreement with [75].

MVC	MUs	RoA	Sensitivity	Precision	CoV	MDR [Hz]
10%	42.12 ± 2.74	0.83 ± 0.22	0.99 ± 0.03	0.84 ± 0.22	0.23 ± 0.11	15.41 ± 3.70
30%	29.48 ± 5.27	0.95 ± 0.13	1.00 ± 0.02	0.95 ± 0.13	0.18 ± 0.07	21.44 ± 8.03
50%	23.48 ± 2.63	0.97 ± 0.10	1.00 ± 0.03	0.97 ± 0.10	0.16 ± 0.05	23.21 ± 8.09

Table 1: Decomposition results on the simulated HDsEMG data. The reported numbers are the average of five runs, grouped by the MVC level. The scores consist of the mean and standard deviation.

MVC	Running Time [s]
10%	809.27 ± 69.00
30%	813.22 ± 17.13
50%	1092.42 ± 17.68

Table 2: Average running time (in seconds) of the KmCKC algorithm, grouped by the MVC level, and averaged over five runs.

With regards to other studies proposing decomposition methods, it is difficult to compare the obtained results to them as each uses different data, often not publicly available. The only piece of research that incorporated the same simulated recordings is the one that actually published them as well [12]. The major difference is that the authors added noise of various levels on top of the raw signals. Nevertheless, some parallels can be still drawn between the results, particularly by analysing the scores with the least amount of added noise, which in this case is 30 dB Signal-to-Noise Ratio (SNR). The work in [12] evaluates two algorithms: the introduced GSS method and the gCKC algorithm. In terms of the number of identified sources, KmCKC managed to extract slightly more units for 30% and 50% MVCs and substantially more for 10% contraction force. The sensitivity of GSS is a bit worse than KmCKC (0.92), although it reports better precision values (0.98). The gCKC seems to be more balanced in this matter, reporting on average 0.96 and 0.94 for sensitivity and precision respectively. The CoV values obtained by GSS are considerably better as they are around 0.13. Overall, the highlighted differences between the performance of the algorithms in [12] and KmCKC here are considered to be within acceptable ranges. Most of the scores are on average very close, except for the KmCKC numbers obtained for 10% MVC data, which perhaps reveals a weakness of this particular algorithm. In other words, the performance of the replicated KmCKC method appears to be in agreement with other methods as per [12] for 30% and 50% MVC levels but delivers poorer outcomes on 10% MVC signals.

In terms of running time, as presented in Table 2, the algorithm took around 13.5 minutes to decompose either 10% or 30% MVC cases (16 seconds data samples), raising to 18.2 minutes in the other setting. This longer time for the latter case can perhaps be explained by more frequent discharge firings, resulting in more spikes for the algorithm to process. A similar trend can be observed in [12], where the GSS method is actually a bit slower than KmCKC presented here, even for 30 dB SNR cases (a range of 18.3 - 21.6 minutes). This shows the replicated KmCKC technique

falls within expected runtime boundaries.

Given the provided results on decomposed simulated data and the brief comparison with [12], the overall performance of the replicated method can be considered relatively good as all the reported evaluation metrics fall within reasonable values. On top of that, the KmCKC procedure appears to be fairly less complicated than other decomposition algorithms, which was also considered when choosing the method to replicate. It is also worth pointing out that, although the runtime of the implemented procedure is indeed within expected boundaries, it is still too long to be considered for online decomposition tasks, although it could be hypothesised that the separation vectors could be computed offline and then utilised in real-time to transform recordings into sources. Nevertheless, this aspect is a common property shared among most of such algorithms, which has been specifically tackled in some works (e.g. [42, 43, 44]). The other disadvantage is the non-deterministic nature of KmCKC, requiring the data to be processed multiple times to obtain reliable outcomes, effectively raising overall runtime substantially. In terms of the replication process itself, it turned out to be extremely difficult, consuming more of the project’s time than anticipated. Fortunately, despite the challenges, the method has been delivered and given the validation results, the entire replication task is therefore considered successful.

5 Joint Analysis of HDsEMG and EEG

After the successful completion of the implementation phase, the project progressed to the final stage that involved processing the real experimental recordings. This part of the work incorporated all the components of the employed methodology, as thoroughly described in Section 3. The entire process, also depicted in Figure 9, started with simultaneously recorded EEG and HDsEMG signals during the performance of the two types of hand movements (pinch and grip), followed by data pre-processing of both datasets. The HDsEMG data were then processed by the adopted decomposition procedure (see Section 5.1), comprising pre-processing, KmCKC algorithm and post-processing. The obtained sources were then subject to further processing in order to find the MUs active across multiple trials (Section 5.2). All these preliminary steps finally enabled the generation of EEG ERPs (Section 5.3), followed by the analysis (Section 5.4).

5.1 Decomposition

The experimental HDsEMG recordings were decomposed on a trial-by-trial basis. An alternative approach of processing combined trials within a given session was also explored, but it resulted in lower quality sources obtained. The entire three-stage decomposition process (i.e., pre-processing, decomposition, and post-processing) was employed to extract the underlying motor units from the data. As part of the preliminary steps, a few channels were discarded from each participant after manual inspection of the recordings and their power spectra (a range of 1-9 channels). The observations were then extended ($K = 16$) and whitened. The KmCKC algorithm decomposed signals into IPTs using the following parameters: $N_{mdl} = 350$, $r = 5$,

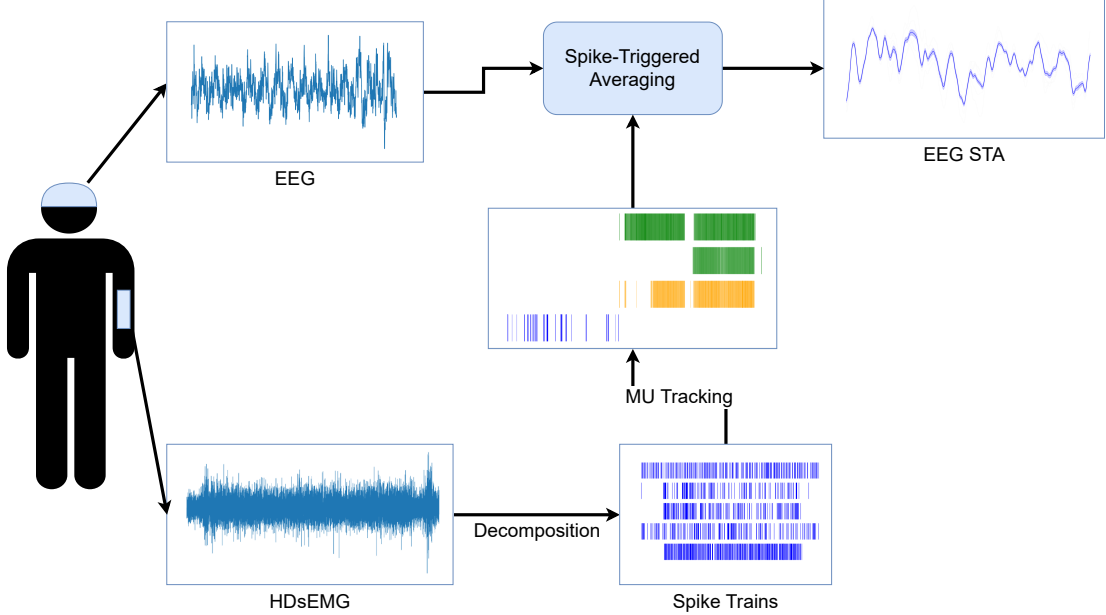


Figure 9: Entire pipeline of components involved in the analysis. First, both EEG and HDsEMG recordings were simultaneously collected according to the experimental protocol. HDsEMG signals were then decomposed into MU spike trains using the KmCKC algorithm. Next, the identified sources were tracked across subsequent trials, which were then used in conjunction with EEG to form EEG event-related potentials.

$N_p = 5$, $h = 40$, $\varphi_{nc} = 60$. The method was run 5 times to improve reliability of the results, aggregating the outcomes into a single set. Furthermore, the spike trains were extracted by first squaring the obtained IPTs and then applying a threshold equal to three standard deviations of the squared signal. At this point, the quality metrics were calculated. Only the sources satisfying a set standard were used in further analysis, that is, those characterised by $CoV_{ISI} < 0.3$ (90% accuracy [75]) and MDR in the range of 6 and 40 Hz. Then, the similarity score was calculated between each pair of remained spike trains as per Equation (17). Any pair exceeding a threshold of 0.1 was considered the same, in which case the source with a lower CoV_{ISI} value was retained. Lastly, the timings of the peaks were corrected based on the time lag obtained from the estimated MUAP shapes, as per the description in Section 3.2.4. Overall, 225 unique motor units were extracted across all five subjects. A more detailed assessment of the outcomes are provided in Tables 3 and 4. The results in this form were further processed by the MU tracking part.

5.2 Common Sources

The motor units extracted from each individual contraction were further processed to identify the same sources active across subsequent trials but within one session. As described in Section 3.1.2, every session consisted of six repetitions of each of the two movements, performed in randomised order, hence giving 12 trials per session. Since the decomposition was performed separately for each trial, the common MUs were tracked across each set of 12 decomposition results. Moreover, the tracking was intentionally done across the sources relating to both movement types in order to

Subject	MUs (pinch/grip)	Pulses	CoV	MDR [Hz]
S04	93 (10/83)	312.57 ± 78.26	0.22 ± 0.05	12.34 ± 3.09
S05	9 (0/9)	209.00 ± 45.72	0.23 ± 0.07	8.27 ± 1.81
S06	36 (18/18)	251.17 ± 61.67	0.20 ± 0.06	9.94 ± 2.44
S07	87 (34/53)	313.14 ± 95.59	0.24 ± 0.05	12.37 ± 3.78
S08	0 (0/0)	N/A	N/A	N/A

Table 3: Summary of the sources extracted from the experimental HDsEMG signals for each subject. The MUs column provides the total amount of identified units as well as the source count per each movement type. The other three columns, namely, Pulses (average number of peaks across the MUs), CoV, and MDR, are given as the mean and standard deviation. No sources were identified for subject S08 (this was the participant for whom only two sessions were recorded).

Movement Type	MUs	Pulses	CoV	MDR [Hz]
grip	163	317.01 ± 86.95	0.23 ± 0.05	12.52 ± 3.43
pinch	62	251.00 ± 66.32	0.22 ± 0.06	9.92 ± 2.62

Table 4: The statistics of motor units extracted from HDsEMG recordings, grouped by each hand movement type.

identify not only the MUs active at either the grip or pinch movement but also the ones present in both situations. As a consequence, the tracked sources were categorised depending on which type of movement it was found to be active in: a) pinch, b) grip, and c) mixed (denoting the sources active in both types of contractions). Furthermore, only the sources active in at least two trials were used in further analysis, discarding the ones present in only one contraction. The alpha levels used in the *ISCTEST* tracking method that refer to false positive and false discovery rates were both set to 0.001. Overall, after processing each subjects' session separately, 46 common sources were identified. A detailed view on the results are presented in Tables 5 and 6. An example of tracked sources shown in the form of spike trains is demonstrated in Figure 10.

Subject	MUs			
	Mixed	Grip	Pinch	Total
S04	3	17	1	21
S05	0	3	0	3
S06	5	2	1	8
S07	2	6	6	14

Table 5: The amount of common sources found categorised by their type and grouped by subjects.

Source Type	MUs	Pulses
grip	28	1095.39 ± 582.78
pinch	8	670.25 ± 348.16
mixed	10	1375.10 ± 745.17

Table 6: The number of tracked MUs with regards to the type of movement they consist of. Mixed type denotes a source active during both types of movement.

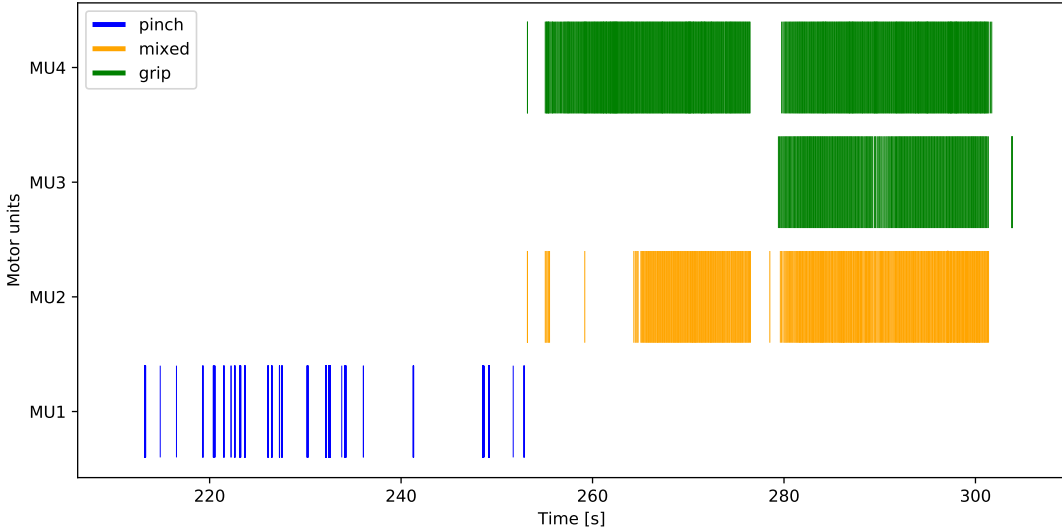


Figure 10: A representative example of motor units tracked across consecutive repetitions. As indicated by different colors, some sources were found to be active in only one type of movement, whereas one unit was identified in both, denoted as mixed.

5.3 EEG Event-Related Potentials

The combined spike trains from the MU tracking procedure were utilised to build spike-triggered EEG ERPs, with the spikes used as triggers. The EEG signals were concatenated within each experimental session and according to the order the movements were performed by the volunteers. The time instants of the spike trains were then used to identify EEG epochs, which start at 1.0 second before and end 0.2 seconds after the triggering spike, with a baseline correction applied to the first 200 ms (see Section 3.5 for details). Epochs were then averaged across epochs belonging to a specific motor unit and an EEG channel of interest. Moreover, in the hope of making potential anomalies in EEG ERPs even more prominent, the mean of the epochs of the four neighbouring EEG channels was subtracted from the epoch belonging to the channel of interest when calculating the averages. In addition, for visualisation purposes and easier analysis, the actual plots of the averages were limited to the period starting at 0.4 seconds before and ending at 0.2 seconds after the event. All 46 common sources identified were used in this way to generate 46 separate ERPs, which were then further analysed.

Although it is common in the ERP literature to show grand averages of ERPs, that is, ERPs averaged also across participants, given the specifics of this project we do

not expect a common ERP to be present, so the results were analysed on a per-participant basis. Some of the most interesting results are presented in the following paragraphs.

Firstly, as presented in Figure 11, it has been observed that in many cases the ERPs originating from the motor cortex area opposite to the used hand (contralateral) are in better agreement with each other than those from the other side of the motor area. This can be noticed not only in the depicted ERPs, but also in each channel's average signal and its standard error after applying the Laplacian filtering. In other words, lower error levels confirm higher synchronisation of the signals.

Secondly, some examples also demonstrated quite different phases of the waveforms between the two sides of the motor area (see Figure 12). Interestingly, the phases were often found to be exactly opposite.

Furthermore, hardly any consistent ERPs were identified that would occur anywhere near the expected time lag from the triggering event (around 15 ms before). This applies to sessions within and across the subjects. The only example that would fit the requirements was located in a grip-only source at 19 ms before the trigger (see Figure 13).

No significant difference in ERPs was observed neither between the three types of sources nor among the grip-only and pinch-only ones. Example ERPs of a source active during the pinch movement only is presented in Figure 14.

5.4 Discussion

Decomposition. Out of the five participants, the recordings from four of them were successfully decomposed. The highest number of motor units was extracted from the data of subjects S04 and S07 (93 and 87 sources, respectively), followed by S06 with 36 sources. Very few MUs were identified for S05 (9 units), while none of the sources extracted from S08 signals passed the quality filters, so this participant was excluded from further analysis. The MUs obtained from S06 and S07 appear to be the most balanced with regards to the type of sources extracted (pinch or grip), whereas subjects S04 and S05 seem to be skewed towards grip-based MUs. Furthermore, the spike trains obtained from S04 and S07 are characterised by a higher number of pulses involved, which is in line with higher MDR values. The regularity of all the spikes seems to be within similar boundaries, with the most regular ones found in S06 ($CoV_{ISI} = 0.20$). In general, a higher number of grip-related MUs were identified, which could be because this movement type likely recruits more muscles and involves a slightly higher force hence activating more motoneurons, so there are more sources to identify. This fact is partly supported by higher MDR values and spike counts found in grip-related sources. The regularity of spikes was on average the same across both types.

Given 60 movement repetitions overall performed by subjects 4–7 (2 movements × 6 repetitions × 5 sessions), the mean number of extracted sources per each trial is almost 1 (0.99), though the amount varied greatly on a trial-by-trial basis (a range of 0–6). Perhaps the closest study these results can be compared to is the one presented

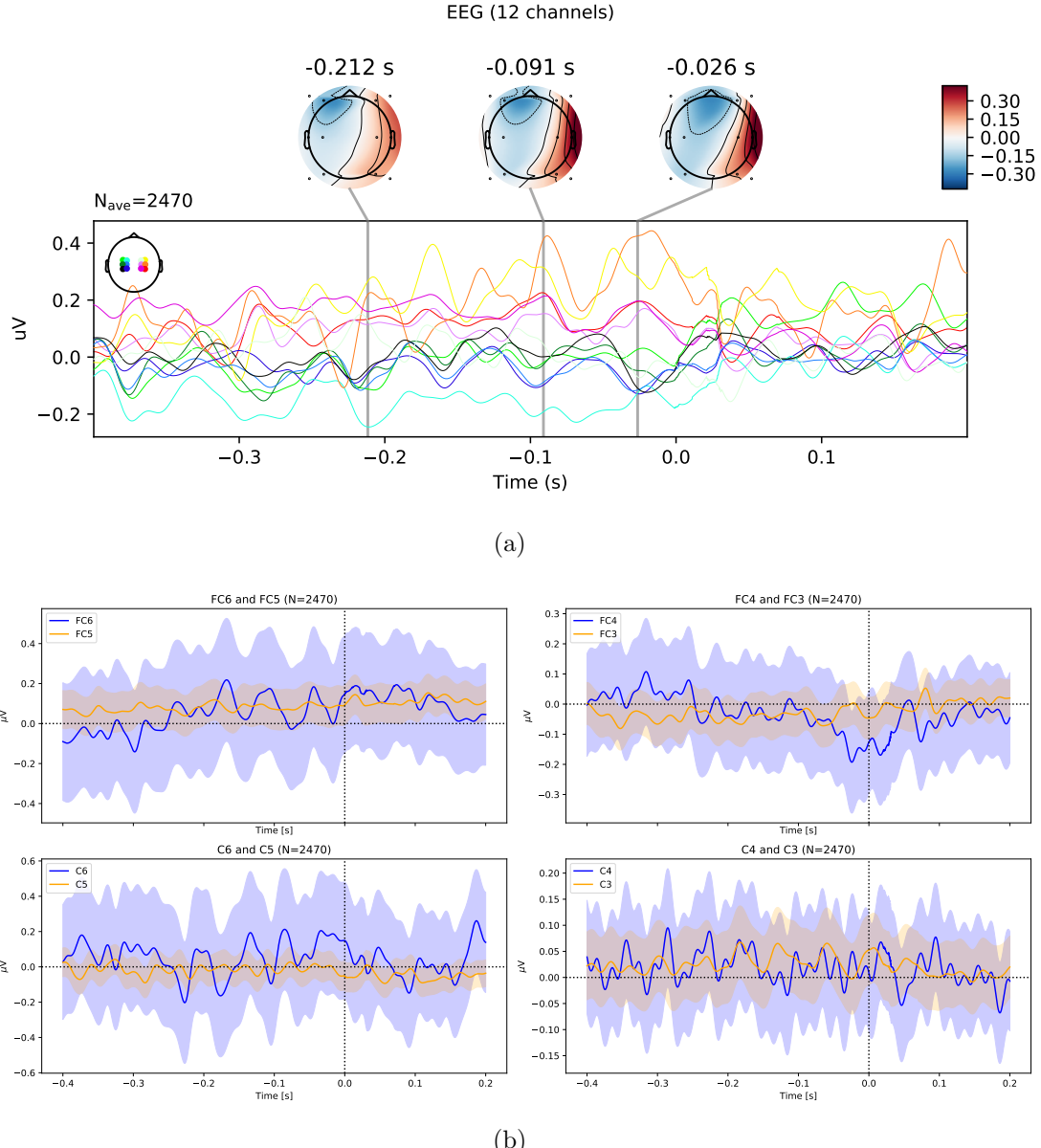


Figure 11: Example ERPs of a mixed source showing higher synchronisation in the contralateral motor cortex, specifically throughout 200 ms before the triggering event at time lag zero (subfigure (a)). Better synchronisation is also reflected in lower levels of the standard error (shaded areas) in the orange curves (subfigure (b)), which show each channel's mean after the Laplacian filtering.

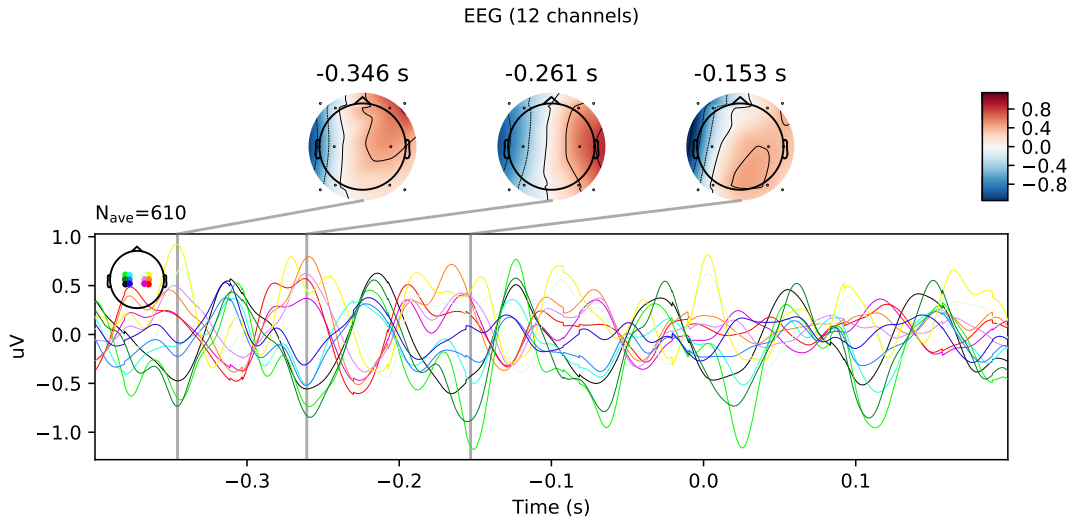


Figure 12: Example ERPs of a mixed source presenting the opposite signal phases between two hemispheres of the activated motor cortex area.

in [39], where two of the investigated finger combinations, namely, index and grasp, can relate to those studies as part of this project (pinch and grip respectively) with a particular focus on the extensor muscles. The major difference is, however, that the study in [39] investigated sinusoidal contractions, as opposed to isometric ones in this work. The authors incorporated the classic CKC algorithm to decompose the HDsEMG recordings, applied to each trial separately as well. They also used some quality metrics to discard some low-quality results. More precisely, they used the PNR score with a threshold corresponding to 70% accuracy, which is in contrast to this study that used CoV_{ISI} with a threshold of 0.3 corresponding to an accuracy of 90%. Furthermore, the lower bound of acceptable MDR values in [39] was set to 2 Hz, accepting as a consequence more sparse sources than this project (lower MDR set to 6 Hz). On top of that, the authors admit the spike trains were afterwards inspected and manually corrected to account for clear false positive and false negative peaks. This clearly shows that the work in [39] used more relaxed quality metrics, allowing for some lower quality results and manually correcting the outputs, which again shows the current decomposition methods are not fully automated. Thus, given those post-processing details, it is not so surprising that the authors report a higher number of identified sources, 7.7 and 5.9 for grasp and index, respectively, although the fact that they also obtained more MUs for grasp than the other movement is in line with the results obtained here. Given the discrepancies in the defined quality boundaries between [39] and this work, differences in the number of extracted sources are also anticipated. In fact, the quality measures utilised here were intentionally set to a very high standard as only the sources of the highest quality can be further used to calculate the EEG ERPs.

Common Sources. When it comes to the commonly identified sources, most of them were found for subjects S04 and S07 (21 and 14 sources, respectively), which is unsurprising given the highest percentage of the normal motor units were overall extracted

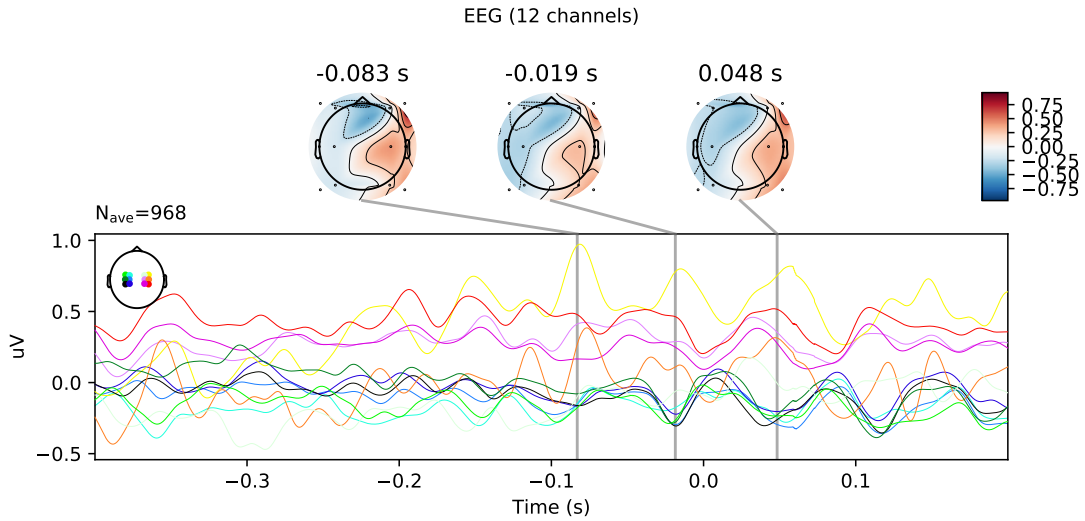


Figure 13: Example ERPs of a grip-only source including an ERP around the time lag of interest, which in this case points at -19 ms.

for those two. Furthermore, 8 MUs were tracked for subject S06, followed by only 3 for subject S05. All three types of sources, namely, pinch, grip and mixed, were successfully found in all subjects except for S05, which included only sources for the grip movement. The majority of grip-related units can be clearly attributed to S04, while the pinch-only ones to S07. Overall, the sources related to the grip movement constituted the majority, in fact, more than the other two types combined, which again is likely due to more grip sources found in the decomposition stage. With regards to the spike count of commonly identified units, the mixed sources clearly dominate (1375 spikes), whereas the pinch ones are on average only half as long (670 spikes). This is partly expected as pinch-only MUs have lower MDR frequencies and hence are more sparse. It is true that mixed sources consists of both types of MUs, but due to higher rates of MDR in the grip ones, mixed sources can be dominated by them and have higher spike counts as a consequence. On the other hand, this could also suggest that pinch-only common sources on average consist of a lower amount of spike trains, that is, they were found to be active in less trials. This conclusion can be further generalised to other source types, suggesting that the mixed MUs are on average active in the highest number of contractions overall.

With regards to the tracking procedure itself, establishing a working method was considerably challenging. Interestingly, such a technique is seemingly used by multiple studies, but the descriptions of steps taken are usually very brief and not enough to replicate the approach. Given the scarcity of the articles that propose tracking techniques and thoroughly explain them at the same time, it is rather non-trivial to implement and use such a method.

EEG ERPs. The obtained ERPs on average seem to be more synchronised in the motor area contralateral to the used hand, as indicated by concurring signals and lower standard error levels. This is in agreement with other studies [5, 61, 64] that reported

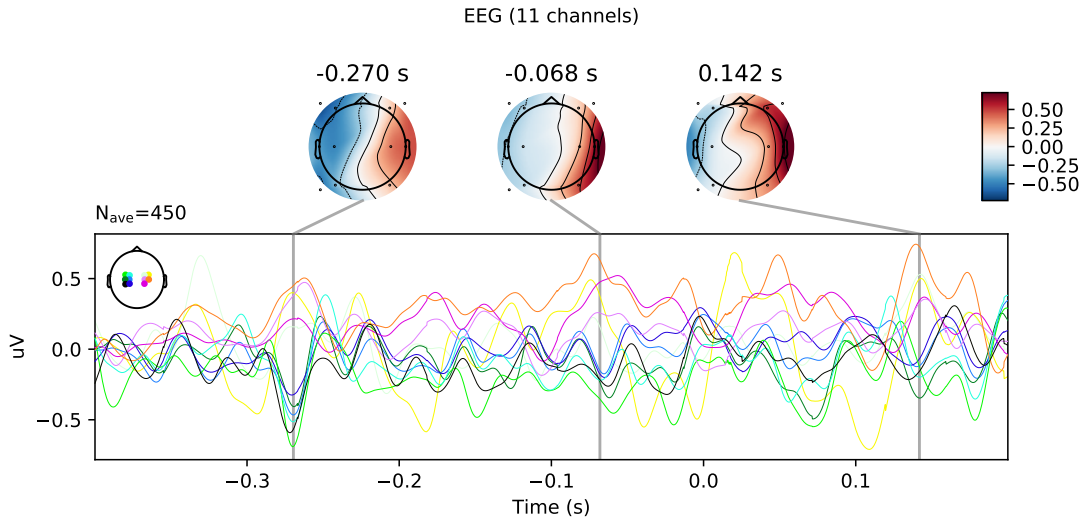


Figure 14: Example ERPs of a finger-only source. Higher synchronisation and an opposite signal phase can be observed in the contralateral motor area. Channel CP6 has been discarded due to high noise levels.

significant increase in motor cortex activity opposite to the used limb. At times, the synchronisation was found to be the strongest specifically during 200 ms before the triggering event, suggesting this period is of special importance for corticomuscular coupling. The appearance of the opposite phases between the ERPs originating from different sides of the motor area are, on the other hand, more difficult to explain. What is clear, however, is that it shows yet another difference between the hemispheres. It also shows that a clear synchronisation is not necessarily exclusive to the contralateral area, but can be present bilaterally. If this is the case, the opposite phases may in fact be more important.

According to the literature, the expected delay between the activity of the fingers as collected from the forearm and the originating cortical signals should be approximately at 15 ms [64]. Thus, we would expect any interesting ERPs related to the studied hand movements near this lag region. Given the results obtained, only a single ERP was found near this lag (19 ms, see Figure 13). Some more ERPs were identified in the lag region of 30 ms, but this rather goes beyond the anticipated range. However, the lack of found ERPs does not necessarily imply they are not there but may rather reflect the difficulty of detecting them. This is because the ERPs of interest have very low amplitudes and hence require very high accuracy of the other methods used in the entire processing in order to be discovered. One obvious place of possible errors is definitely the decomposition algorithm as inaccurately identified discharge times directly contribute to less clear ERPs. In fact, the validation performed in Section 4.3 showed that the replicated method, although delivering good results overall, performed the worst on 10% MVC recordings. As the HDsEMG experimental signals were of 10% MVC as well, it could be the obtained spike trains are not accurate enough. It is also worth pointing out that the spike train alignment procedure modifies the timings of the peaks, which can also be a source of errors. The other reason of undetected

ERPs might be the MU tracking part as it is entirely possible some motor units were incorrectly recognised as the same, resulting in different sources used as one to generate ERPs. Furthermore, it is possible that some interesting anomalies are actually happening in other brain areas, outside of the motor cortex. This could be because some past research reported also other brain regions to be activated specifically when performing fine finger control [62, 63]. Lastly, the investigated hand gestures may simply be too difficult, or not informative enough, to find the said ERPs within them, suggesting to look at other hand manipulations.

Given the lack of consistent and significant ERPs detected, it is difficult to notice any clear differences between the two types of hand movements, at least within this particular setup. A relatively small number of the tracked motor units also does not help (46), especially since merely 8 of them belong to the pinch-only group, most of which have a rather low number of spikes and hence low quality ERPs. This is perhaps a good demonstration that not only the quality of the extracted spike trains matters, but also how many of them can be identified by a given decomposition algorithm. Many of the sources initially obtained from the decomposition were not found to be active in more than one trial, resulting in many potential MUs lost in the tracking stage. Finally, revisiting the conclusions reached in the previous paragraph, it could be the case the inspected hand movements are too difficult to process effectively for the purpose of this type of analysis.

6 Discussion

This study consisted of two main phases: a) the replication and validation of the KmCKC decomposition algorithm, and b) the joint analysis of HDsEMG and EEG signals, both of which were discussed in detail in Sections 4 and 5 respectively. The first stage was directly related to the research question Q1 and the goal G1. Among many state-of-the-art decomposition methods, the KmCKC algorithm was chosen to be replicated, partly due to its relatively lower complexity, but mainly because of the performance it offers while being a fairly automated method. As it turned out later on, a decomposition algorithm is not the only necessary ingredient in the entire HDsEMG decomposition process. The required pre- and post-processing steps appeared to be equally challenging as the algorithm itself, especially the latter. However, any further analysis, which was the subject of the second phase of the project, would not have been possible without a working HDsEMG decomposition procedure. For this reason, the first stage of the project consumed much more time than initially anticipated, requiring to abandon some interesting ideas we originally wanted to investigate. Fortunately, despite the encountered challenges (see Section 4.1), the method was finally replicated, meeting the objective O1.

Furthermore, the implementation was validated against obtained simulated HDsEMG data that were specifically prepared to test decomposition algorithms. This type of publicly available data appears to be a highly scarce resource within the field, making the replication and validation of said algorithms considerably more difficult. Though it is worth mentioning that invasive recordings seem to be more broadly accessible,

either real data with ground truth [86] or data generation frameworks [87]. In fact, the initial plan of this project included the use of both aforementioned invasive data to validate the implemented method, however, as the project progressed, it appeared the CKC-based methods can operate exclusively on surface signals [10].

Nevertheless, the implementation of the KmCKC method was successfully validated, confirming the accuracy of the replication and hence fulfilling the objective O2 and goal G1. When it comes to the research question Q1, the details of the identified challenges within HDsEMG decomposition were thoroughly discussed in Section 4.1. In brief, the majority of the issues were caused by inconsistencies in the literature and the need to decipher vague descriptions of the algorithms. Also, the decomposition methods in their workings are in general relatively complicated, making it difficult to build the intuition about their internal parts and effectively correct inevitable implementation errors made at some point. The difficulty of obtaining a reliable and suitable testing dataset also negatively contributes to the process. It is believed that some of the aforementioned problems could be resolved through some further work, for instance, by providing more careful and informative method descriptions in order to unveil the secrets of HDsEMG decomposition, or simply by a more open attitude of sharing the code and the data [88]. This study humbly strives to contribute to this positive direction.

The second and final stage of the project involved work contributing to the goal G2 in order to answer research questions Q2 and Q3. As part of the first objective within this goal (O3), the experimental HDsEMG recordings were decomposed into the underlying sources using the replicated KmCKC algorithm. This dataset was clearly more challenging compared to the simulated signals. Both the quality and the amount of extracted motor units varied across participants, but overall fulfilling the objective. Although it could be argued the overall decomposition quality could be improved, perhaps by exploring other state-of-the-art algorithms [28, 10].

The next step (objective O4) was about tracking the MUs active in multiple subsequent trials within a given session. Apart from the sources present in a specific movement type, some of them were identified in both gestures within the same session. Only 8 common sources were identified exclusively in the pinch movement, considerably limiting further analysis about the characteristics unique to fine finger control. Perhaps extracting more MUs via decomposition would improve this situation. It could be also that this specific muscle contraction is just inherently very difficult to process and extract reliable sources from. The quality of the tracking procedure can also be questioned, which is however rather tricky to evaluate in any other way than manual inspection of the results it provides. As manual investigation of every single tracking result is not a solution, some further work might be needed here to thoroughly test such methods. Employing an entirely different tracking method could also help [79].

Finally, the last two objectives, O5 and O6, were fulfilled by generating the ERPs and carefully analysing them, reaching the goal G2. With regards to the question Q2, we were not able to detect any consistent ERPs in motor cortex that would arise in close proximity (15 ms) before the triggering spikes. The simplest explanation is that there

is nothing there to be actually discovered. On the other hand, it could be because such ERPs are extremely difficult to detect, blaming the quality of the preceding methods involved in the pipeline and thus encouraging to try other decomposition and tracking procedures. A third interpretation could be that the ERPs of interest exist in other brain areas, outside of motor cortex, as suggested by [62, 63]. When it comes to the question Q3, we posed a hypothesis that the difference between primal and fine hand movements could be reflected by, for instance, different ERP timings. Unfortunately, given the lack of consistent ERPs, this hypothesis cannot be validated. Moreover, the further analysis of general characteristics of the produced EEG waveforms did not reveal any significant discrepancies between the two movement types. This analysis was, however, hampered by a relatively low number of ERPs related exclusively to fine motor control, which, again, encourages to look at other decomposition and tracking methods in the hope of getting higher quality results. Though a simple answer that there is in fact no significant difference between them still applies. Lastly, similarly to the situation with the ERPs, it could be that more prominent discrepancies are present out of motor cortex area.

7 Conclusions and Future Work

In conclusion, this project investigated modern HDsEMG decomposition methods in order to study single motor units and their associated EEG ERPs that correspond to primal and fine hand movements. The replication process of the selected decomposition method was extremely challenging due to various inconsistencies in the literature, particularly with regards to additional steps necessary before and after the decomposition phase. Despite the setbacks, the KmCKC algorithm was successfully implemented and validated against simulated HDsEMG signals. It was then used to decompose experimental HDsEMG recordings that were jointly collected with EEG data. The extracted motor units were then tracked across subsequent trials to form longer and more reliable spike trains. Finally, the ERPs were obtained through spike-triggered averaging and analysed accordingly.

Provided the ERPs produced specifically in this setup, almost none of them were detected in the time period (15 ms) preceding the triggering event, across all subjects. Likewise, no significant difference was revealed in the ERPs between the sources representing fine and primal hand movements. This could either indicate no such differences exist in the motor cortex or reflect the limitations of the incorporated methods, including the fact that HDsEMG decomposition detects only superficial motor units close to the surface of the skin. Thus, given possible further improvements, we believe the two aspects of detecting specific ERPs and potential discrepancies between primal and fine finger movements remain open, including the eventuality of identifying them in other brain areas.

When it comes to the project itself, all the set goals and objectives are considered to have been reached, though they changed slightly as the work progressed. The three research questions posed as a consequence of recognised gaps have also been answered, though there is clearly more work that can be done as a follow-up of this study. The

project was managed through Jira (task management) and regular consultations with the supervisors. The code was regularly committed to a designated GitLab repository where all of the developed components are now available¹.

It is fair to admit that the implementation of the decomposition-related modules consumed more time than initially anticipated and hence limited some of the original plans of the project, though these can be still pursued as part of the follow-up work. This partly happened because of the complexity of the studied methods, but also due to the nature of research in general. Thus, it was very difficult to predict every detail of the project before reaching its certain stage, inevitably leading to changing plans. This perhaps is unavoidable in this type of projects and can be considered an integral part of research, which was a really valuable lesson to learn.

Furthermore, it has been also observed how truly important it is to share the code and data, in science and in general, as the lack of these aspects makes the replication process considerably more challenging and prone to errors. Although it has been pointed out throughout this document how the decomposition literature is not detailed enough, the experience of describing these very methods as part of this report gave a chance to acknowledge how challenging this task actually is. Complex methods are indeed difficult to understand and eventually replicate, but perhaps even more demanding to accurately explain them in relatively simple terms. Therefore, regardless of the mentioned algorithmic descriptions, it is fair to admit that HDsEMG decomposition methods are just inherently highly complicated, requiring many complex components to work properly, not to mention the difficulty of testing them and fixing eventual implementation flaws.

Another concluding remark is that generating consistent and reliable ERPs is definitely non-trivial as they require highly accurate data obtained from preceding modules. On top of that, having such a complicated pipeline of components, it is rather difficult to locate the malfunctioning pieces badly affecting the resulting ERPs. The analysis of said ERPs constitutes quite a challenge as well, mostly because they can vary substantially across participants. Thus, it is at times very difficult to categorise a located anomaly as either a true underlying process or just a difference purely caused by physiological differences between subjects.

There are many interesting avenues through which this study can be advanced. First of all, given the downsides of K-means algorithm, incorporating other, more robust, clustering techniques could in theory improve the stability of the KmCKC, ideally eliminating the need to run it multiple times on the same data samples. Of particular interest could be OPTICS [89] and DBSCAN [90], both of which are deterministic and allow for more complex clusters shapes.

Furthermore, it would be interesting to replicate more decomposition methods and compare them to KmCKC. This could involve some of the most popular methods, such as gCKC [28] and the algorithm presented in [10]. This idea could be taken even further to develop a publicly accessible environment where many decomposition methods would be evaluated against various datasets, allowing to add more methods

¹URL of the repository: https://cseegit.essex.ac.uk/2019_ce901/ce901_machlanski_d

and data in the future through a shared interface between algorithms. This thought is specifically inspired by SpikeForest [91] and SpikeInterface [92], that provide a shared environment and an interface respectively to evaluate spike sorting algorithms. In addition, to help with testing and data scarcity within HDsEMG decomposition, it could be useful to provide a data generation framework, something similar to what MEArec [87] provides for spike sorting community.

Moreover, provided how little attention is given to source tracking within HDsEMG community, it might be beneficial to investigate these methods more closely. Perhaps a procedure combining both MUAP shapes and extracted independent components (or mixing matrices) could be an interesting approach to consider.

With regards to EEG ERPs and the inspected hand movements, it could be that the differences are more prominent in other brain areas. In fact, the work in [62, 63] shows that fine finger control requires not only motor cortex, but also other brain regions, suggesting an interesting direction for future work. Finally, it could be that the currently inspected hand movements are too similar to each other in terms of hand manipulation complexity, suggesting to investigate other movement types. This could perhaps involve gestures beyond a simple force application, such as holding a pen (fine control) and holding a suitcase (simple force).

8 References

- [1] C. Xiang, V. Lantz, W. Kong-Qiao, Z. Zhang-Yan, Z. Xu, and Y. Ji-Hai, “Feasibility of building robust surface electromyography-based hand gesture interfaces,” in *2009 Annual International Conference of the IEEE Engineering in Medicine and Biology Society*, pp. 2983–2986, Sept. 2009.
- [2] D. Farina, H. Rehbaum, A. Holobar, I. Vujaklija, N. Jiang, C. Hofer, S. Salminger, H.-W. van Vliet, and O. C. Aszmann, “Noninvasive, Accurate Assessment of the Behavior of Representative Populations of Motor Units in Targeted Reinnervated Muscles,” *IEEE Transactions on Neural Systems and Rehabilitation Engineering*, vol. 22, pp. 810–819, July 2014.
- [3] D. Farina, N. Jiang, H. Rehbaum, A. Holobar, B. Graimann, H. Dietl, and O. C. Aszmann, “The Extraction of Neural Information from the Surface EMG for the Control of Upper-Limb Prostheses: Emerging Avenues and Challenges,” *IEEE Transactions on Neural Systems and Rehabilitation Engineering*, vol. 22, pp. 797–809, July 2014.
- [4] “Dexterous Transradial Osseointegrated Prosthesis with neural control and sensory feedback — DeTOP Project — H2020 — CORDIS — European Commission.” <https://cordis.europa.eu/project/id/687905>.
- [5] B. A. Conway, D. M. Halliday, S. F. Farmer, U. Shahani, P. Maas, A. I. Weir, and J. R. Rosenberg, “Synchronization between motor cortex and spinal motoneuronal pool during the performance of a maintained motor task in man.,” *The Journal of Physiology*, vol. 489, pp. 917–924, Dec. 1995.

- [6] J. Wessberg, “Private communication,” Sept. 2017.
- [7] D. Farina, R. Merletti, and R. M. Enoka, “The extraction of neural strategies from the surface EMG: An update,” *Journal of Applied Physiology*, vol. 117, pp. 1215–1230, Dec. 2014.
- [8] A. Holobar and D. Zazula, “Multichannel Blind Source Separation Using Convolution Kernel Compensation,” *IEEE Transactions on Signal Processing*, vol. 55, pp. 4487–4496, Sept. 2007.
- [9] Y. Ning, X. Zhu, S. Zhu, and Y. Zhang, “Surface EMG Decomposition Based on K-means Clustering and Convolution Kernel Compensation,” *IEEE Journal of Biomedical and Health Informatics*, vol. 19, pp. 471–477, Mar. 2015.
- [10] F. Negro, S. Muceli, A. M. Castronovo, A. Holobar, and D. Farina, “Multi-channel intramuscular and surface EMG decomposition by convolutive blind source separation,” *Journal of Neural Engineering*, vol. 13, p. 026027, Apr. 2016.
- [11] T. Kapelner, I. Vujaklija, N. Jiang, F. Negro, O. C. Aszmann, J. Principe, and D. Farina, “Predicting wrist kinematics from motor unit discharge timings for the control of active prostheses,” *Journal of NeuroEngineering and Rehabilitation*, vol. 16, p. 47, Apr. 2019.
- [12] M. R. Mohebian, H. R. Marateb, S. Karimimehr, M. A. Mañanas, J. Kranjec, and A. Holobar, “Non-invasive Decoding of the Motoneurons: A Guided Source Separation Method Based on Convolution Kernel Compensation With Clustered Initial Points,” *Frontiers in Computational Neuroscience*, vol. 13, p. 14, 2019.
- [13] R. Merletti, A. Holobar, and D. Farina, “Analysis of motor units with high-density surface electromyography,” *Journal of Electromyography and Kinesiology*, vol. 18, pp. 879–890, Dec. 2008.
- [14] R. Merletti, M. Aventaggiato, A. Botter, A. Holobar, H. Marateb, and T. M. M. Vieira, “Advances in surface EMG: Recent progress in detection and processing techniques,” *Critical Reviews in Biomedical Engineering*, vol. 38, no. 4, pp. 305–345, 2010.
- [15] D. Farina, A. Holobar, R. Merletti, and R. M. Enoka, “Decoding the neural drive to muscles from the surface electromyogram,” *Clinical Neurophysiology*, vol. 121, pp. 1616–1623, Oct. 2010.
- [16] E. Martinez-Valdes, C. M. Laine, D. Falla, F. Mayer, and D. Farina, “High-density surface electromyography provides reliable estimates of motor unit behavior,” *Clinical Neurophysiology*, vol. 127, pp. 2534–2541, June 2016.
- [17] A. Del Vecchio, A. Holobar, D. Falla, F. Felici, R. M. Enoka, and D. Farina, “Tutorial: Analysis of motor unit discharge characteristics from high-density surface EMG signals,” *Journal of Electromyography and Kinesiology*, vol. 53, p. 102426, Aug. 2020.

- [18] D. Farina, M.-F. Lucas, and C. Doncarli, “Optimized Wavelets for Blind Separation of Nonstationary Surface Myoelectric Signals,” *IEEE Transactions on Biomedical Engineering*, vol. 55, pp. 78–86, Jan. 2008.
- [19] M. Gazzoni, D. Farina, and R. Merletti, “A new method for the extraction and classification of single motor unit action potentials from surface EMG signals,” *Journal of Neuroscience Methods*, vol. 136, pp. 165–177, July 2004.
- [20] G. R. Naik, D. K. Kumar, S. P. Arjunan, M. Palaniswami, and R. Begg, “Limitations and Applications of ICA for Surface Electromyogram,” in *2006 International Conference of the IEEE Engineering in Medicine and Biology Society*, pp. 5739–5742, Aug. 2006.
- [21] M. Chen and P. Zhou, “A Novel Framework Based on FastICA for High Density Surface EMG Decomposition,” *IEEE transactions on neural systems and rehabilitation engineering : a publication of the IEEE Engineering in Medicine and Biology Society*, vol. 24, pp. 117–127, Jan. 2016.
- [22] A. Hyvarinen, “Fast and robust fixed-point algorithms for independent component analysis,” *IEEE Transactions on Neural Networks*, vol. 10, pp. 626–634, May 1999.
- [23] M. Chen, X. Zhang, X. Chen, and P. Zhou, “Automatic Implementation of Progressive FastICA Peel-Off for High Density Surface EMG Decomposition,” *IEEE Transactions on Neural Systems and Rehabilitation Engineering*, vol. 26, pp. 144–152, Jan. 2018.
- [24] M. Chen, X. Zhang, Z. Lu, X. Li, and P. Zhou, “Two-Source Validation of Progressive FastICA Peel-Off for Automatic Surface EMG Decomposition in Human First Dorsal Interosseous Muscle,” *International Journal of Neural Systems*, vol. 28, p. 1850019, Nov. 2018.
- [25] A. Holobar and D. Zazula, “Correlation-based decomposition of surface electromyograms at low contraction forces,” *Medical and Biological Engineering and Computing*, vol. 42, pp. 487–495, July 2004.
- [26] D. Zazula and A. Holobar, “An approach to surface EMG decomposition based on higher-order cumulants,” *Computer Methods and Programs in Biomedicine*, vol. 80, pp. S51–S60, Dec. 2005.
- [27] C. Disselhorst-Klug, G. Rau, A. Schmeer, and J. Silny, “Non-invasive detection of the single motor unit action potential by averaging the spatial potential distribution triggered on a spatially filtered motor unit action potential,” *Journal of Electromyography and Kinesiology: Official Journal of the International Society of Electrophysiological Kinesiology*, vol. 9, pp. 67–72, Feb. 1999.
- [28] A. Holobar and D. Zazula, “Gradient Convolution Kernel Compensation Applied to Surface Electromyograms,” in *Independent Component Analysis and Signal Separation* (M. E. Davies, C. J. James, S. A. Abdallah, and M. D. Plumley, eds.), Lecture Notes in Computer Science, (Berlin, Heidelberg), pp. 617–624, Springer, 2007.

- [29] A. Holobar and D. Zazula, “On the selection of the cost function for gradient-based decomposition of surface electromyograms,” in *2008 30th Annual International Conference of the IEEE Engineering in Medicine and Biology Society*, pp. 4668–4671, Aug. 2008.
- [30] A. Holobar, D. Farina, M. Gazzoni, R. Merletti, and D. Zazula, “Estimating motor unit discharge patterns from high-density surface electromyogram,” *Clinical Neurophysiology: Official Journal of the International Federation of Clinical Neurophysiology*, vol. 120, pp. 551–562, Mar. 2009.
- [31] A. Holobar, M. A. Minetto, A. Botter, F. Negro, and D. Farina, “Experimental analysis of accuracy in the identification of motor unit spike trains from high-density surface EMG,” *IEEE transactions on neural systems and rehabilitation engineering: a publication of the IEEE Engineering in Medicine and Biology Society*, vol. 18, pp. 221–229, June 2010.
- [32] H. R. Marateb, K. C. McGill, A. Holobar, Z. C. Lateva, M. Mansourian, and R. Merletti, “Accuracy assessment of CKC high-density surface EMG decomposition in biceps femoris muscle,” *Journal of Neural Engineering*, vol. 8, p. 066002, Oct. 2011.
- [33] R. Istenic, A. Holobar, R. Merletti, and D. Zazula, “EMG Based Muscle Force Estimation using Motor Unit Twitch Model and Convolution Kernel Compensation,” in *11th Mediterranean Conference on Medical and Biomedical Engineering and Computing 2007* (T. Jarm, P. Kramar, and A. Zupanic, eds.), IFMBE Proceedings, (Berlin, Heidelberg), pp. 114–117, Springer, 2007.
- [34] A. Holobar, V. Glaser, J. A. Gallego, J. L. Dideriksen, and D. Farina, “Non-invasive characterization of motor unit behaviour in pathological tremor,” *Journal of Neural Engineering*, vol. 9, p. 056011, Sept. 2012.
- [35] J. Benito-León, J. I. Serrano, E. D. Louis, A. Holobar, J. P. Romero, P. Povalej-Bržan, J. Kranjec, F. Bermejo-Pareja, M. D. del Castillo, I. J. Posada, and E. Rocon, “Essential tremor severity and anatomical changes in brain areas controlling movement sequencing,” *Annals of Clinical and Translational Neurology*, vol. 6, pp. 83–97, Nov. 2018.
- [36] A. Holobar, J. A. Gallego, J. Kranjec, E. Rocon, J. P. Romero, J. Benito-León, J. L. Pons, and V. Glaser, “Motor Unit-Driven Identification of Pathological Tremor in Electroencephalograms,” *Frontiers in Neurology*, vol. 9, 2018.
- [37] V. Glaser and A. Holobar, “On the impact of spike segmentation on motor unit identification in dynamic surface electromyograms,” in *2017 39th Annual International Conference of the IEEE Engineering in Medicine and Biology Society (EMBC)*, pp. 430–433, July 2017.
- [38] J. Ting, A. Del Vecchio, D. Friedenberg, M. Liu, C. Schoenewald, D. Sarma, J. Collinger, S. Colachis, G. Sharma, D. Farina, and D. J. Weber, “A wearable neural interface for detecting and decoding attempted hand movements in a per-

- son with tetraplegia,” in *2019 41st Annual International Conference of the IEEE Engineering in Medicine and Biology Society (EMBC)*, pp. 1930–1933, July 2019.
- [39] S. Tanzarella, S. Muceli, A. Del Vecchio, A. Casolo, and D. Farina, “Non-invasive analysis of motor neurons controlling the intrinsic and extrinsic muscles of the hand,” *Journal of Neural Engineering*, July 2020.
- [40] M. Chen, A. Holobar, X. Zhang, and P. Zhou, “Progressive FastICA Peel-Off and Convolution Kernel Compensation Demonstrate High Agreement for High Density Surface EMG Decomposition,” *Neural Plasticity*, vol. 2016, p. 3489540, 2016.
- [41] M. Šavc, V. Glaser, J. Kranjec, I. Cikajlo, Z. Matjačić, and A. Holobar, “Comparison of Convulsive Kernel Compensation and Non-Negative Matrix Factorization of Surface Electromyograms,” *IEEE Transactions on Neural Systems and Rehabilitation Engineering*, vol. 26, pp. 1935–1944, Oct. 2018.
- [42] V. Glaser, A. Holobar, and D. Zazula, “Real-Time Motor Unit Identification From High-Density Surface EMG,” *IEEE Transactions on Neural Systems and Rehabilitation Engineering*, vol. 21, pp. 949–958, Nov. 2013.
- [43] D. Y. Barsakcioglu, M. Bracklein, A. Holobar, and D. Farina, “Control of Spinal Motoneurons by Feedback from a Non-invasive Real-Time Interface,” *IEEE Transactions on Biomedical Engineering*, pp. 1–1, 2020.
- [44] C. Chen, S. Ma, X. Sheng, D. Farina, and X. Zhu, “Adaptive real-time identification of motor unit discharges from non-stationary high-density surface electromyographic signals,” *IEEE Transactions on Biomedical Engineering*, pp. 1–1, 2020.
- [45] Y. Ning, S. Zhu, X. Zhu, and Y. Zhang, “A hybrid multi-channel surface EMG decomposition approach by combining CKC and FCM,” in *2013 6th International IEEE/EMBS Conference on Neural Engineering (NER)*, pp. 335–338, Nov. 2013.
- [46] H. Jinbao, Y. Xinhua, L. Zaifei, L. Guojun, and Z. Shiguan, “The decomposition of multi-channel surface electromyogram based on waveform clustering convolution kernel compensation,” in *2015 Chinese Automation Congress (CAC)*, pp. 979–982, Nov. 2015.
- [47] Y. Liu, Y. Ning, S. Li, P. Zhou, W. Z. Rymer, and Y. Zhang, “Three-dimensional innervation zone imaging from multi-channel surface EMG recordings,” *International journal of neural systems*, vol. 25, p. 1550024, Sept. 2015.
- [48] Y. Peng, J. He, B. Yao, S. Li, P. Zhou, and Y. Zhang, “Motor Unit Number Estimation Based on High-Density Surface Electromyography Decomposition,” *Clinical neurophysiology : official journal of the International Federation of Clinical Neurophysiology*, vol. 127, pp. 3059–3065, Sept. 2016.
- [49] J. He and Z. Luo, “A simulation study on the relation between the motor unit depth and action potential from multi-channel surface electromyography recordings,” *Journal of Clinical Neuroscience*, vol. 54, pp. 146–151, Aug. 2018.

- [50] G. Garcia, R. Okuno, and K. Azakawa, “A decomposition algorithm for surface electrode-array electromyogram,” *IEEE Engineering in Medicine and Biology Magazine*, vol. 24, pp. 63–72, July 2005.
- [51] C. J. De Luca, A. Adam, R. Wotiz, L. D. Gilmore, and S. H. Nawab, “Decomposition of Surface EMG Signals,” *Journal of Neurophysiology*, vol. 96, pp. 1646–1657, Sept. 2006.
- [52] S. H. Nawab, S.-S. Chang, and C. J. De Luca, “High-yield decomposition of surface EMG signals,” *Clinical Neurophysiology*, vol. 121, pp. 1602–1615, Oct. 2010.
- [53] Y. Ning, Y. Zhao, A. Juraboev, P. Tan, J. Ding, and J. He, “Multichannel Surface EMG Decomposition Based on Measurement Correlation and LMMSE,” *Journal of Healthcare Engineering*, vol. 2018, June 2018.
- [54] A. K. Clarke, S. F. Atashzar, A. Del Vecchio, D. Y. Barsakcioglu, S. Muceli, P. Bentley, F. Urh, A. Holobar, and D. Farina, “Deep Learning for Robust Decomposition of High-Density Surface EMG Signals,” *IEEE transactions on biomedical engineering*, vol. PP, July 2020.
- [55] S. P. Arjunan and D. K. Kumar, “Decoding subtle forearm flexions using fractal features of surface electromyogram from single and multiple sensors,” *Journal of NeuroEngineering and Rehabilitation*, vol. 7, p. 53, Oct. 2010.
- [56] G. R. Naik and D. K. Kumar, “Identification of Hand and Finger Movements Using Multi Run ICA of Surface Electromyogram,” *Journal of Medical Systems*, vol. 36, pp. 841–851, Apr. 2012.
- [57] T. Kapelner, F. Negro, O. C. Aszmann, and D. Farina, “Decoding Motor Unit Activity From Forearm Muscles: Perspectives for Myoelectric Control,” *IEEE Transactions on Neural Systems and Rehabilitation Engineering*, vol. 26, pp. 244–251, Jan. 2018.
- [58] B. Potočnik, M. Divjak, F. Urh, A. Frančič, J. Kranjec, M. Šavc, I. Cikajlo, Z. Matjačić, M. Zadravec, and A. Holobar, “Estimation of Muscle Co-Activations in Wrist Rehabilitation After Stroke is Sensitive to Motor Unit Distribution and Action Potential Shapes,” *IEEE Transactions on Neural Systems and Rehabilitation Engineering*, vol. 28, pp. 1208–1215, May 2020.
- [59] C. Chen, G. Chai, W. Guo, X. Sheng, D. Farina, and X. Zhu, “Prediction of finger kinematics from discharge timings of motor units: Implications for intuitive control of myoelectric prostheses,” *Journal of Neural Engineering*, vol. 16, p. 026005, Jan. 2019.
- [60] J. R. Rosenberg, A. M. Amjad, P. Breeze, D. R. Brillinger, and D. M. Halliday, “The Fourier approach to the identification of functional coupling between neuronal spike trains,” *Progress in Biophysics and Molecular Biology*, vol. 53, no. 1, pp. 1–31, 1989.

- [61] P. Brown, S. Salenius, J. C. Rothwell, and R. Hari, “Cortical Correlate of the Piper Rhythm in Humans,” *Journal of Neurophysiology*, vol. 80, pp. 2911–2917, Dec. 1998.
- [62] M. J. Catalan, M. Honda, R. A. Weeks, L. G. Cohen, and M. Hallett, “The functional neuroanatomy of simple and complex sequential finger movements: A PET study,” *Brain: A Journal of Neurology*, vol. 121 (Pt 2), pp. 253–264, Feb. 1998.
- [63] R. Kawashima, M. Matsumura, N. Sadato, E. Naito, A. Waki, S. Nakamura, K. Matsunami, H. Fukuda, and Y. Yonekura, “Regional cerebral blood flow changes in human brain related to ipsilateral and contralateral complex hand movements—a PET study,” *The European Journal of Neuroscience*, vol. 10, pp. 2254–2260, July 1998.
- [64] J. Gross, P. A. Tass, S. Salenius, R. Hari, H. J. Freund, and A. Schnitzler, “Cortico-muscular synchronization during isometric muscle contraction in humans as revealed by magnetoencephalography,” *The Journal of Physiology*, vol. 527 Pt 3, pp. 623–631, Sept. 2000.
- [65] B. Hellwig, S. Häussler, B. Schelter, M. Lauk, B. Guschlbauer, J. Timmer, and C. H. Lücking, “Tremor-correlated cortical activity in essential tremor,” *Lancet (London, England)*, vol. 357, pp. 519–523, Feb. 2001.
- [66] F. Negro and D. Farina, “Linear transmission of cortical oscillations to the neural drive to muscles is mediated by common projections to populations of motoneurons in humans,” *The Journal of Physiology*, vol. 589, no. 3, pp. 629–637, 2011.
- [67] J. A. Gallego, J. L. Dideriksen, A. Holobar, J. Ibáñez, J. L. Pons, E. D. Louis, E. Rocon, and D. Farina, “Influence of common synaptic input to motor neurons on the neural drive to muscle in essential tremor,” *Journal of Neurophysiology*, vol. 113, pp. 182–191, Jan. 2015.
- [68] M. R. Mohebian, H. R. Marateb, S. Karimimehr, M. A. Mañanas, J. Kranjec, and A. Holobar, “Simulated High-Density Surface Electromyographic signals for the validation of decomposition algorithms,” Mar. 2019.
- [69] D. Farina and R. Merletti, “A novel approach for precise simulation of the EMG signal detected by surface electrodes,” *IEEE Transactions on Biomedical Engineering*, vol. 48, pp. 637–646, June 2001.
- [70] J. Thomas, Y. Deville, and S. Hosseini, “Time-domain fast fixed-point algorithms for convolutive ICA,” *IEEE Signal Processing Letters*, vol. 13, pp. 228–231, Apr. 2006.
- [71] D. Steinley, “K-means clustering: A half-century synthesis,” *British Journal of Mathematical and Statistical Psychology*, vol. 59, no. 1, pp. 1–34, 2006.
- [72] A. Holobar, M. A. Minetto, and D. Farina, “Accurate identification of motor unit discharge patterns from high-density surface EMG and validation with a

novel signal-based performance metric,” *Journal of Neural Engineering*, vol. 11, p. 016008, Jan. 2014.

- [73] C. Pouzat, O. Mazor, and G. Laurent, “Using noise signature to optimize spike-sorting and to assess neuronal classification quality,” *Journal of Neuroscience Methods*, vol. 122, pp. 43–57, Dec. 2002.
- [74] R. Q. Quiroga, Z. Nadasdy, and Y. Ben-Shaul, “Unsupervised spike detection and sorting with wavelets and superparamagnetic clustering,” *Neural Computation*, vol. 16, pp. 1661–1687, Aug. 2004.
- [75] X. Hu, N. L. Suresh, B. Jeon, H. Shin, and W. Z. Rymer, “Statistics of inter-spike intervals as a routine measure of accuracy in automatic decomposition of surface electromyogram,” in *2014 36th Annual International Conference of the IEEE Engineering in Medicine and Biology Society*, pp. 3541–3544, Aug. 2014.
- [76] R. Beck, C. Houtman, M. O’Malley, M. Lowery, and D. Stegeman, “A technique to track individual motor unit action potentials in surface EMG by monitoring their conduction velocities and amplitudes,” *IEEE Transactions on Biomedical Engineering*, vol. 52, pp. 622–629, Apr. 2005.
- [77] E. M. Maathuis, J. Drenthen, J. P. van Dijk, G. H. Visser, and J. H. Blok, “Motor unit tracking with high-density surface EMG,” *Journal of Electromyography and Kinesiology*, vol. 18, pp. 920–930, Dec. 2008.
- [78] A. Hyvärinen, “Testing the ICA mixing matrix based on inter-subject or inter-session consistency,” *NeuroImage*, vol. 58, pp. 122–136, Sept. 2011.
- [79] E. Martinez-Valdes, F. Negro, C. M. Laine, D. Falla, F. Mayer, and D. Farina, “Tracking motor units longitudinally across experimental sessions with high-density surface electromyography,” *The Journal of Physiology*, vol. 595, pp. 1479–1496, Mar. 2017.
- [80] A. Hyvärinen and P. Ramkumar, “Testing Independent Component Patterns by Inter-Subject or Inter-Session Consistency,” *Frontiers in Human Neuroscience*, vol. 7, 2013.
- [81] P. Virtanen, R. Gommers, T. E. Oliphant, M. Haberland, T. Reddy, D. Cournapeau, E. Burovski, P. Peterson, W. Weckesser, J. Bright, S. J. van der Walt, M. Brett, J. Wilson, K. Jarrod Millman, N. Mayorov, A. R. J. Nelson, E. Jones, R. Kern, E. Larson, C. Carey, İ. Polat, Y. Feng, E. W. Moore, J. VanderPlas, D. Laxalde, J. Perktold, R. Cimrman, I. Henriksen, E. A. Quintero, C. R. Harris, A. M. Archibald, A. H. Ribeiro, F. Pedregosa, P. van Mulbregt, and S. . . Contributors, “SciPy 1.0: Fundamental algorithms for scientific computing in python,” *Nature Methods*, vol. 17, pp. 261–272, 2020.
- [82] T. E. Oliphant, *A Guide to NumPy*, vol. 1. Trelgol Publishing USA, 2006.
- [83] F. Pedregosa, G. Varoquaux, A. Gramfort, V. Michel, B. Thirion, O. Grisel, M. Blondel, P. Prettenhofer, R. Weiss, V. Dubourg, J. Vanderplas, A. Pas-
sos, D. Cournapeau, M. Brucher, M. Perrot, and E. Duchesnay, “Scikit-learn:

- Machine learning in Python,” *Journal of Machine Learning Research*, vol. 12, pp. 2825–2830, 2011.
- [84] J. D. Hunter, “Matplotlib: A 2D Graphics Environment,” *Computing in Science Engineering*, vol. 9, pp. 90–95, May 2007.
- [85] A. Gramfort, M. Luessi, E. Larson, D. A. Engemann, D. Strohmeier, C. Brodbeck, R. Goj, M. Jas, T. Brooks, L. Parkkonen, and M. Hämäläinen, “MEG and EEG data analysis with MNE-Python,” *Frontiers in Neuroscience*, vol. 7, 2013.
- [86] N. Malesevic, A. Björkman, G. S. Andersson, A. Matran-Fernandez, L. Citi, C. Cipriani, and C. Antfolk, “A database of multi-channel intramuscular electromyogram signals during isometric hand muscles contractions,” *Scientific Data*, vol. 7, pp. 1–12, Jan. 2020.
- [87] A. P. Buccino and G. T. Einevoll, “MEArec: A fast and customizable testbench simulator for ground-truth extracellular spiking activity,” *bioRxiv*, p. 691642, Mar. 2020.
- [88] L. A. Celi, L. Citi, M. Ghassemi, and T. J. Pollard, “The PLOS ONE collection on machine learning in health and biomedicine: Towards open code and open data,” *PLOS ONE*, vol. 14, pp. 1–7, Jan. 2019.
- [89] M. Ankerst, M. M. Breunig, H.-P. Kriegel, and J. Sander, “Optics: Ordering points to identify the clustering structure,” *SIGMOD Rec.*, vol. 28, p. 49–60, June 1999.
- [90] M. Ester, H.-P. Kriegel, J. Sander, and X. Xu, “A density-based algorithm for discovering clusters in large spatial databases with noise,” in *Proceedings of the Second International Conference on Knowledge Discovery and Data Mining*, KDD’96, p. 226–231, AAAI Press, 1996.
- [91] J. F. Magland, J. J. Jun, E. Lovero, A. J. Morley, C. L. Hurwitz, A. P. Buccino, S. Garcia, and A. H. Barnett, “SpikeForest: Reproducible web-facing ground-truth validation of automated neural spike sorters,” *bioRxiv*, p. 2020.01.14.900688, Jan. 2020.
- [92] A. P. Buccino, C. L. Hurwitz, J. Magland, S. Garcia, J. H. Siegle, R. Hurwitz, and M. H. Hennig, “SpikeInterface, a unified framework for spike sorting,” *bioRxiv*, p. 796599, Oct. 2019.